McGill

Department of Mining &
Materials Engineering

McGill University
College of Engineering
Mining and Materials Engineering
August 2017

Dynamic transformation of $\alpha \rightarrow \beta$ at temperatures below the β-transus in commercially pure titanium.

By

Anes Foul

Department of Mining and Materials Engineering
McGill University
Montreal, Canada

August 2017

A Thesis Submitted to the Faculty of Graduate Studies and Research in Partial Fulfillment of the Requirements for the Degree of Master of Engineering

Abstract

The concept of dynamic transformation was first discovered in steels in the late 1980s. Yada and co-workers showed that austenite can be transformed into ferrite by deformation at temperatures above the Ae3 (transformation temperature). Recently, various researchers around the world have proposed explanations of this unusual phenomenon. This is important in controlling and modelling the microstructure generated after deformation. The deformation behavior of commercially pure titanium grade 2 during hot working was previously studied by many researchers. For different titanium and titanium alloys, an increase in the β volume fraction by deforming at temperatures below the β-transus is observed. Here the driving force for transformation is taken as the flow stress difference between the work hardened alpha and the yield stress of the fresh beta that takes its place. Koike et al. (2000) showed an increase in β volume fraction after hot deformation below the β-transus on a Ti-5.5 wt%Al-1.5 wt%Fe alloy. This was also observed in the work of Xu et al. (2010) where high sub-tranus softening was observed in CP Ti grade 2. Jonas et al. (2017) also showed that this phenomenon was observed on three titanium alloys including a near α titanium (IMI834) alloy. Finally, Aranas and the current author (2017) explained the thermodynamic behavior behind this unusual phenomenon in CP Ti grade 2. In the present work, compression tests at temperatures between 750 and 970 ^{o}C were performed to determine the experimental driving force, dependence of the β volume fraction produced on deformation temperature, and the minimum temperature to induce dynamic transformation in CP Ti grade 2.

Résume

Le concept de transformation dynamique a d'abord été découvert dans les aciers à la fin des années 1980. Yada et ses collègues ont montré que l'austénite peut être transformée en ferrite par déformation à des températures supérieures à Ae3 (température de transformation). Récemment, divers chercheurs du monde ont proposé des explications sur ce phénomène inhabituel. Ceci est important pour contrôler et modéliser la microstructure générée après déformation. Le comportement de déformation du titane grade 2 commercialement pur pendant le travail à chaud a été étudié précédemment par de nombreux chercheurs. Pour différents alliages de titane, on observe une augmentation de la fraction de volume β par déformation à des températures inférieures au β-transus. Ici, la force motrice de la transformation est considérée comme la différence de contrainte d'écoulement entre l'alpha durci durci et le stress élastique de la bêta fraîche qui prend sa place. Koike et al. (2010) ont observé une augmentation de la fraction de volume ß après une déformation à chaud en dessous du β-transus sur un alliage de Fe Ti-5.5 wt% Al-1.5% en poids de Fe. Cela a été appliqué également au travail de Xu et al. (2010) qui ont observés un ramollissement sub-tranus élevé chez CP Ti de la classe 2. Jonas et al. (2016) ont également montré que ce phénomène est observé sur trois titanes comprenant un alliage de titane proche beta (IMI834). Enfin, Aranas et l'auteur actuel (2017) ont expliqué le comportement thermodynamique derrière ce phénomène inhabituel dans la classe 2 de CP Ti. Dans le présent travail, des essais de compression à des températures entre 750 et 970 ºC ont été effectués pour déterminer la force motrice expérimentale, la dépendance de la fraction de volume β produite sur la température de déformation et la température minimale pour induire une transformation dynamique dans le CP Ti de grade 2.

Acknowledgments

There are numerous people whose guidance, inspiration, and unwavering support made this thesis possible. I would be honored to take this moment to express my gratitude and respect for my mentors, colleagues, friends and family who have helped me along the way. First and foremost, I wish to thank my supervisor, Prof. John Jonas and co-supervisor Prof. Stephen Yue for the support, guidance, and wealth of expertise he provided throughout this work. I am very grateful to members of the deformation group at McGill University. In particular, I wish to thank Dr. Clodualdo Aranas and Baoqi Guo for their expertise and feedback throughout my study. I wish to thank Ameth Fall and Muhammad Jahazi from École de technologie supérieure for their collaboration, expertise, and discussions. I am very appreciative of the faculty and staff of the Department of Materials Engineering. I also want to thank Barbara Hanley for her willingness to answer questions and provide insight. I wish to thank the machine shop staff especially Raymond Lemay for their expert services, assistance, and uplifting conversations. I would also like to thank Karan Narang, and Khalid Anwar for their comradery, advice and friendship. I want to thank my family and friends: thank you for your constant encouragement and love. Lastly, I would like to thank NSERC Canada for their contributions to my research.

Preface

The experimental work presented in this thesis was conducted at McGill University within the department of Mining and Materials Engineering. This included all the experimental design, material heat treatments, sample preparation, and metallography. Collaboration with Ameth Fall and Muhammad Jahazi from École de technologie supérieure regarding sample preparation and understanding of dynamic transformation in commercially pure titanium. Chapter 4 and 5 includes the details of this work to be published August 2017.

Table of Contents

List of Figures

Fig. 15 a) to d) shows how α nucleates at grain boundaries and then grows as lamellae into the prior β grain when cooling from the β-transus field of Ti-6Al-4V (high-temperature microscopy).

Fig. 16 Microstructure of Ti-6Al-4V after slow cooling (50 C/h) from a) □ c) □ e), and water quenching from 1050C in b), 800C in d), and 650C in f).

Fig. 17 Equiaxed microstructures of Ti-6Al-4V via recrystallization: a) fine equiaxed; b) coarse equiaxed; c, d) bimodal (OM, TEM).

Fig. 18 Annealing schedule of the machined CP Ti samples

Fig. 19 Schematic of the 100kN MTS compression machine.

Fig. 20 Thermomechanical schedule of the compression tests.

Fig. 21 Stress-strain curves determined at eight different temperatures.

Fig. 22 Optical micrographs show an increase in β-phase formation with increasing deformation temperature.

Fig. 23 Comparison of the beta phase fraction in undeformed and deformed samples.

Fig. 24 The $\boldsymbol{\sigma}\ (\boldsymbol{critical{-}hard\ phase}) - \boldsymbol{\sigma}\ (\boldsymbol{yield{-}soft\ phase})$ for the α → β transformation.

Fig. 25 The driving force for the α → β transformation.

Fig. 26 The minimum temperature to induce DT in CP Tfi Grade 2.

List of Tables

1. Introduction

Energy consumption is a key factor in the metal processing industries. Forging has been used to deform titanium in the past years. Nowadays, many countries are replacing forging by rolling (Fig. 1) to reduce the amount of energy used in the industry and to get better properties at the same time [1]. Countries like Japan, Russia, and USA have already replaced forging by rolling [2-3]. The deformation of titanium by rolling introduces many changes in the microstructure produced and hence the properties. Therefore, studying how to maintain and model the microstructure is an important aspect of the industry [1].

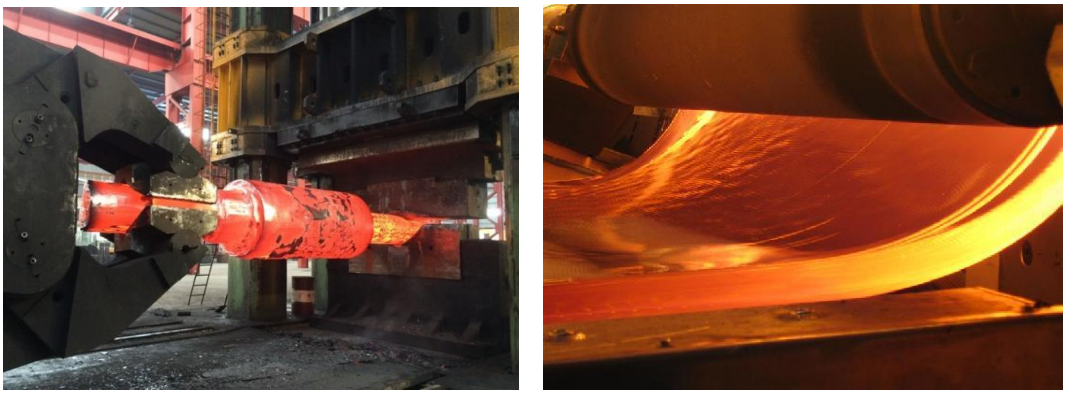

Fig. 1 Typical forging (left) and rolling (right) processes from the industry

Dynamic transformation was first described in steel by Yada and co-workers [4-6]. They noticed that by deforming high strength steel at temperatures above the Ae$_3$ (transformation temperature) some the austenite phase transforms into the ferrite phase as seen in Fig. 2.

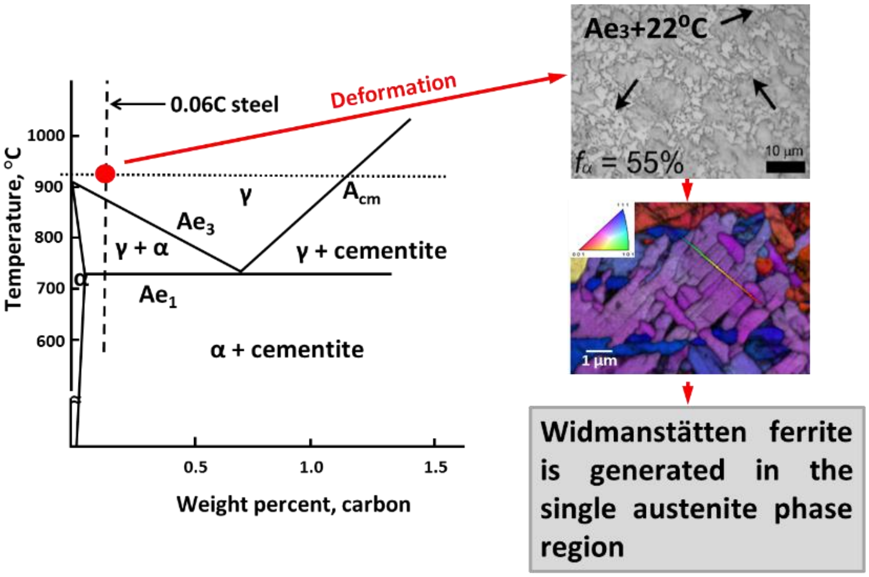

Fig. 2 Fe-C phase diagram where it describes how ferrite is generated in the single phase austenite region [7]

This concept is applied in titanium and titanium alloys and was observed by many researchers in the past few years [8]. In titanium, on the other hand, the transformation is observed when deformation takes place at temperatures below the β-transus where the harder phase α transforms into the softer phase β as shown in Fig 3.

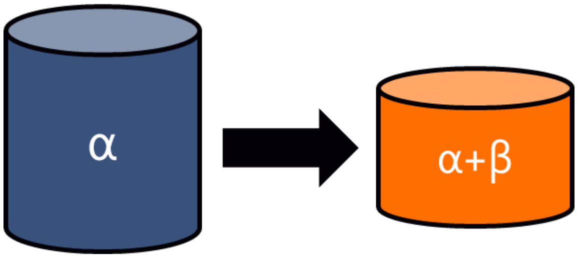

Fig. 3 Deformation in the α single phase region produces α+β phases in CP Ti. [9]

This considerable amount of β formed at temperatures below the β-transus was noticed in the early 2000s by Koike and co-workers [10]. They observed significant increases in the beta volume fraction when samples of Ti- 5.5 wt%Al-1 wt%Fe were strained in tension at temperatures in the range 777 °C to 927 °C [8]. Evidence of dynamic transformation in commercially pure titanium was observed by Xu and co-workers [1]. They observed high sub-transus softening when CP Ti grade 2 was deformed at temperatures below the β-transus (915 °C). They related the softening below the yield stress to dynamic recrystallization DRX where it not possible for DRX to have negative values. This softening is related not only to DRX but also to dynamic transformation where there is a displacive phase change from α to β [9]. Evidence for dynamic transformation was also observed in other titanium and titanium alloys [11-12].

Recently, Aranas and co-workers [8] presented a thermodynamic explanation for dynamic transformation in pure titanium where the driving force for transformation is calculated by the difference between the critical stress of the deformed α phase and the yield stress of the newly formed β phase. In steels, the critical stress is determined using double differentiation [13]. In titanium, on the other hand, this method is not applicable due to the high work hardening rates. Here the critical stress is calculated by equating the driving force with the total energy obstacle. The energy barriers are represented by the free energy difference between β and α and the work of dilatation associated with the transformation. The work of shear accommodation is considered negligible during transformation [8].

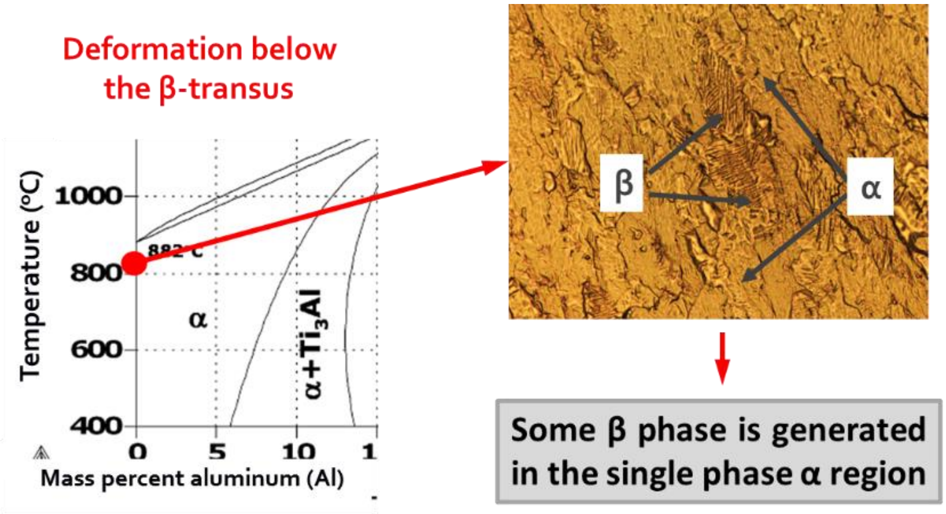

Fig. 4 Ti-Al phase diagram where it shows the formation of β below the β-transus temperature.

In the current work, hot compression tests were carried out on commercially pure titanium grade 2 in a 100 kN MTS machine at temperatures between 750 and 970 ^{o}C with true strain of 0.8 and true strain rate of 0.01 s^{-1}. The proof for dynamic transformation is observed by high sub-transus softening and microstructural evolution. The experimental driving force curve is obtained. The dependence of the β volume fraction produced with deformation temperature is calculated and more than 50% β formation is observed when deformation takes place at 900 ^{o}C. Finally, the minimum temperature to induce dynamic transformation in CP Ti grade 2 is also calculated.

2. Literature review

1. **Metallurgy and characteristics of titanium**

a. Crystal structure

A number of metals including Ca, Fe, Co, Zr, Sn, Ce, Hf and Ti exhibit what is called allotropic transformation. It is where a single material can have different forms of crystal structure depending on the temperature range where one crystal structure is favorable and stable over another. In pure titanium, as well as many titanium alloys, at lower temperatures the material takes the form of the modified hexagonal close packed structure (h.c.p.) called α shown in Fig. 5, and crystallizes into the so-called β titanium, which has the form of body-centered cubic structure (b.c.c.) shown in Fig. 6 at higher temperatures [14]. The allotropic phase transformation in pure titanium (99.8% purity) is at 882°C [15]. The exact transus temperature is very dependent on the interstitial and substitutional elements and therefore the amount of alloying elements [14]. Besides the previously mentioned stable α and β phases some metastable, martensitic type phases (ω, α' and α") may form in titanium alloys when cooled rapidly from the β temperature range. [16, 17] Also indicated in Fig. 5 are the most three densely packed lattice planes, the {0002} plane, one of the three $\{10\bar{1}0\}$ planes, and one of the six $\{10\bar{1}1\}$ planes. The three a_1, a_2, and a_3 axes are the close-packed directions with the indices <$11\bar{2}0$ >. The body centered cubic unit cell (bcc) β phase is also illustrated in Fig. 6 indicating one variant of the six most densely packed {110} lattice planes. The lattice parameter value of pure β titanium at 900°C (a = 0.332 nm) is also indicated. The close-packed directions are the four <111> directions [14].

The hexagonal unit cell of the α phase that is shown in Fig. 5 indicates the room temperature values of the lattice parameters a (0.295 nm) and c (0.468 nm). Because of a small atomic distortion in titanium that results from contraction along the c-axis, the resulting c/a ratio for pure α titanium is 1.587, which is less than the ideal ratio of 1.633 for the hexagonal close-packed crystal structure [18,19]. Also, an increase in the c/a ratio can occur when interstitial atoms such as C, N, O or substitutional α stabilizers with smaller atomic radii than that of titanium are included in the material matrix [17].

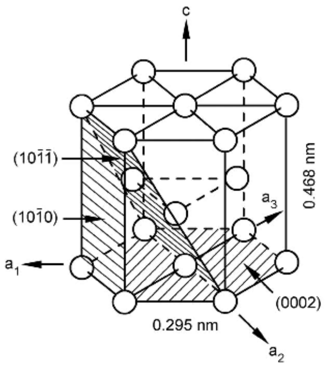

Fig. 5 Unit cell of the α phase.

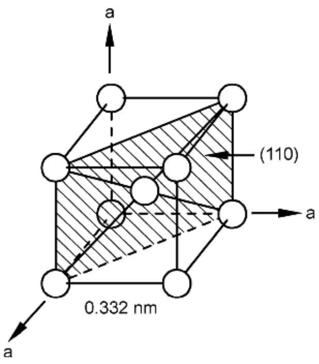

Fig. 6 Unit cell of the β phase.

b. Plastic deformation

The ease of plastic deformation increases from the hexagonal close packed (hcp) lattice to the body-centered cubic (bcc) to the face-centered cubic (fcc) lattice. This phenomenon leads to the explanation of the limited plastic deformability of hcp titanium compared to bcc titanium. Generally, the number of slip systems is only 3 for the hcp structure while it is 12 for the bcc lattice. The planes and directions with highly dense packed atoms are the most energetic and favorable for plastic deformation [14]. The more densely slip planes are packed with atoms, the easier dislocations can glide. Therefore, a packing density of 91% for a slip plane in the hcp lattice should be superior to a slip plane in the bcc lattice with a packing density of only 83%. However, the energy needed for plastic deformation is also directly dependent on the length of the minimal slip path. For hcp lattice structures, the minimum slip path $b_{min}=1\cdot a$, while for bcc structures $b_{min}=0.87\cdot a$, where a is the lattice parameter of the respective unit cell. As a result, plastic deformation of the bcc structure is favorable over that of the hcp structure [14]. A large spacing between prism planes caused by the reduction in the c/a ratio of titanium compared to the ideally packed hexagonal crystal structure leads the packing density of the prism planes to increase relative to the basal plane. This favors slip on prism planes rather than on basal planes. Prism and basal planes have three slip systems each, yet only two are independent of each other, resulting in only four independent slip systems [19].

On the other hand, slip on pyramidal planes does not increase the number further because this type of glide is composed of two prism and basal components and therefore it cannot be considered as an independent slip system. However, according to the von-Mises criterion, at least five independent slip systems are required for the homogeneous plastic deformation of metals. In fact, it is extremely difficult to deform polycrystalline hexagonal titanium. The observed limited ductility is the result of additional deformation on secondary slip systems as well as of possible mechanical twinning [15]. Grain refinement is an effective way of increasing the strength of CP Ti. However, due to the intrinsic characteristics of the HCP structure with few slip systems being activated at room temperature, CP Ti has limited ductility. It is thus necessary to deform CP Ti at higher temperatures at which non-basal slip systems can be activated [22]. The three active slip systems in titanium are depicted in Fig. 7.

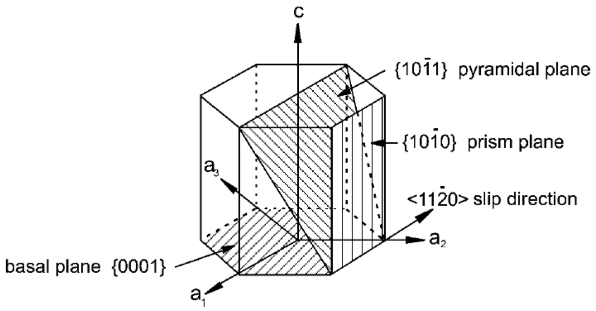

Fig. 7 Slip systems of hexagonal crystal lattices. [15]

c. Deformation Modes

The common mechanisms where by metals respond to plastic deformation involve slip, twinning and stress-induced phase transformations or combinations of the three mechanisms [22]. Hexagonal materials form a class that is extensively used in mechanical and structural applications where the deformation response of the hcp matals and alloys is generally guided by the axial (c/a) ratio. Nevertheless, the deformation behavior of titanium is very complex [18, 22]. The ductile behavior of hexagonal α titanium, especially at low temperatures, results from the activation of twinning deformation modes in addition to conventional slip by dislocations. For CP titanium and some α titanium alloys, these twinning modes are important for the deformation behavior. Although twinning is suppressed nearly completely in two phase α+β alloys by the small phase dimensions, high solute content, and presence of Ti_3Al precipitates, these alloys are quite ductile at low temperatures due to their small phase dimensions. [14] The bcc β phase also permits twinning in addition to slip but the occurrence of twinning in β alloys is limited again to the single phase state and decreases with increasing solute content. In fully heat treated β alloys, which are hardened by the precipitation of α particles, twinning is completely suppressed. In these alloys, twinning can occur during forming before aging can take place. Some commercial β alloys can also form deformation-induced martensite, which further enhances their formability. The formation of such martensite is highly dependent on the alloy composition [15].

1- Slip modes

The various slip planes and slip directions for α titanium are shown in the hexagonal unit cell in Fig. 8. [14] The main slip directions are the three close-packed directions of the type <11$\bar{2}$0 >. The slip planes containing this $\bar{a}$ type of Burgers vector are the (0002) plane, the three {10$\bar{1}$0} planes, and the six {10$\bar{1}$1} planes. Among these three different types of slip planes and with the possible slip directions added to them, there are a total of 12 slip systems [14]. These can be reduced to 8 independent slip systems.

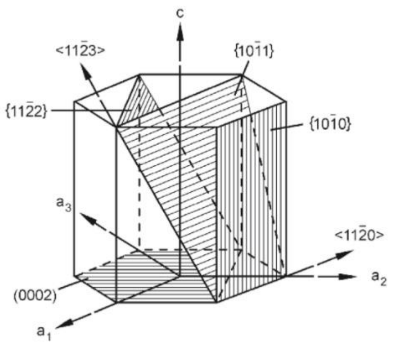

Fig. 8 Slip planes and slip directions in the hexagonal α phase [14]

However, because the shape changes that are produced by the combination of slip system types 1 and 2 from Table 1 are exactly the same as those of slip system type 3, this will lead the number to be further reduced to only 4 independent slip systems. Therefore, assuming the von Mises criterion is correct, which requires at least five independent slip systems for the homogenous plastic deformation of polycrystals, the operation of one of the slip systems with a so-called non-basal Burgers vector needs to be activated, so either the $\bar{c}$ type with the slip direction [0001] or the $\bar{c}$ + $\bar{a}$ type with the slip direction <11$\bar{2}$3 > is required. The presence of $\bar{c}$ + $\bar{a}$ type dislocations has been observed by TEM observation in a number of titanium alloys [18].

Table 1. Slip systems in the hexagonal α phase [14]

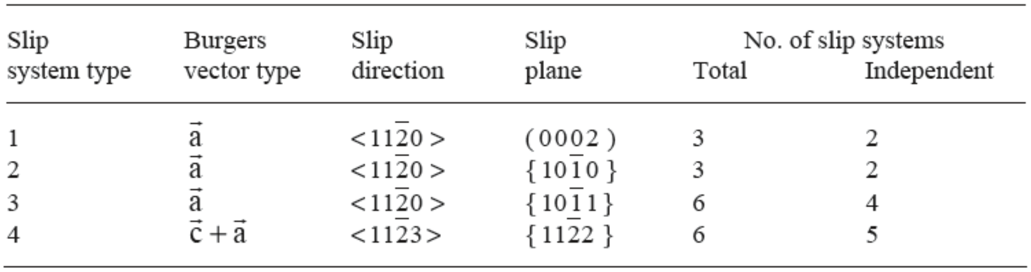

Slip system type	Burgers vector type	Slip direction	Slip plane	No. of slip systems Total	Independent
1	$\vec{a}$	$<11\bar{2}0>$	(0002)	3	2
2	$\vec{a}$	$<11\bar{2}0>$	$\{10\bar{1}0\}$	3	2
3	$\vec{a}$	$<11\bar{2}0>$	$\{10\bar{1}1\}$	6	4
4	$\vec{c}+\vec{a}$	$<11\bar{2}3>$	$\{11\bar{2}2\}$	6	5

The justification for the presence of these $\bar{c} + \bar{a}$ dislocations is not really dependent on whether the von Mises criterion is valid or not, but rather to answer the question which slip systems are activated if a grain in a polycrystalline material is orientated such that the applied stress is in parallel to the c-axis. In that case, neither a slip system with an $\bar{a}$ Burgers vector nor dislocations with a $\bar{c}$ Burgers vector can be activated because the Schmid factor for both is zero. [14]

2- Deformation twinning

The main twinning modes observed in pure titanium are $<10\bar{1}2>$, $<11\bar{2}1>$, and $<11\bar{2}2>$. The crystallographic elements of these twins are listed in Table 2. Twinning modes are especially important for plastic deformation and ductility at low temperatures if the stress axis is parallel to the c-axis and the dislocations with a basal Burgers vector cannot move [19]. The most frequently observed twins are of the $<10\bar{1}2>$ type but they have the smallest twinning shear, as shown in Table 2. Under compression loading parallel to the c-axis, $<11\bar{2}2>$ twins are activated allowing contraction along the c-axis as shown in Fig. 9. After compression loading, $<10\bar{1}1>$ twins were also observed but only at relatively high deformation temperatures above 400°C. Increasing concentrations of solute atoms in α titanium suppress the occurrence of twinning. Although, deformation twinning can cause shape changes, it only plays a major role in pure titanium or in CP titanium where the oxygen concentration is low [14]. On the other hand, Huang et al. [23] studied the microstructural and textural evolution of pure titanium during differential speed rolling and found that twinning only occurs in the initial stages of differential speed rolling (DSR) and that further deformation is dominated by dislocation slip. Finally, Nemat-Nasser el al. also studied the mechanical behavior of CP titanium and found that the density of twins increases markedly with increasing strain rate, strain, and decreasing temperature [19].

Table 2. Twinning elements in α titanium [14]

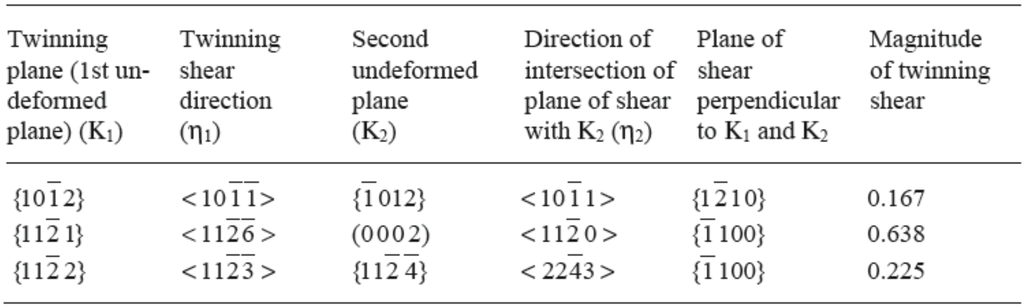

Twinning plane (1st undeformed plane) (K_1)	Twinning shear direction (η_1)	Second undeformed plane (K_2)	Direction of intersection of plane of shear with K_2 (η_2)	Plane of shear perpendicular to K_1 and K_2	Magnitude of twinning shear
$\{10\bar{1}2\}$	$<10\bar{1}\bar{1}>$	$\{\bar{1}012\}$	$<10\bar{1}1>$	$\{1\bar{2}10\}$	0.167
$\{11\bar{2}1\}$	$<11\bar{2}\bar{6}>$	(0002)	$<11\bar{2}0>$	$\{\bar{1}100\}$	0.638
$\{11\bar{2}2\}$	$<11\bar{2}\bar{3}>$	$\{11\bar{2}\bar{4}\}$	$<22\bar{4}3>$	$\{\bar{1}100\}$	0.225

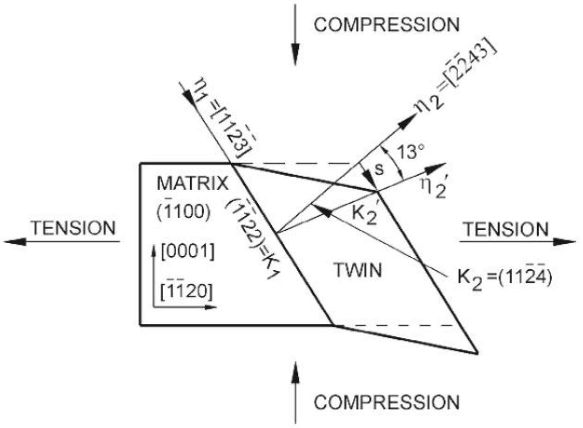

Fig. 9 Shape change produced by {11$\bar{2}$2} twinning [14]

d. Phase diagrams

The alloying elements in titanium are usually classified into α or β stabilizing additions depending on whether they increase or decrease the α/β transformation temperature of 882°C of pure titanium [19,23]. The substitutional element Al and the interstitial elements O, N, and C are all strong α stabilizers and increase the β-transus temperature with increasing solute content, as can be seen from the schematic phase diagram in Fig. 10 Aluminum is the most widely used alloying element in titanium alloys, because it is the only common metal raising the transition temperature and having large solubilities in both the α and β phases. Among the interstitial elements, oxygen can be considered as an alloying element in titanium in those cases where the oxygen content is used to obtain the desired strength level. This is especially true for the different grades of CP titanium. Other α stabilizers include B, Ga, Ge, and the rare earth elements but their solid solubilities are much lower compared to aluminum or oxygen and none of these elements is used commonly as an alloying element [14].

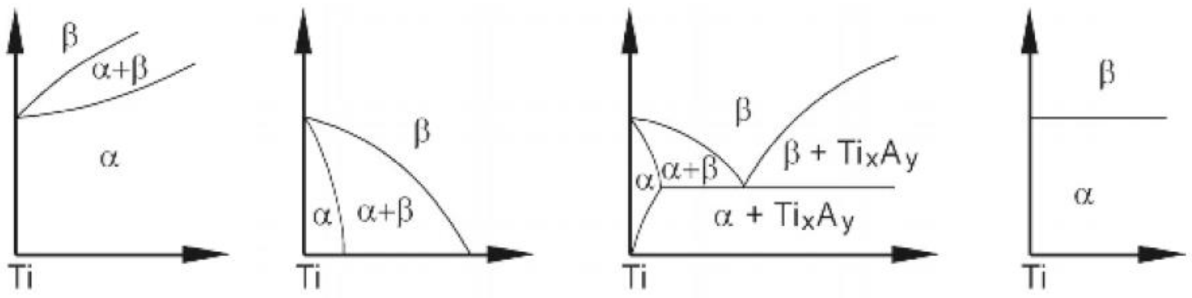

α stabilizer α/β stabilizer neutral

α/β isomorphous α/β eutectoid

(Al,O,N,C) (V,Mo,Nb,Ta) (Fe,Mn,Cr,Ni,Cu,Si,H) (Zr,Sn)

Fig. 10 Effect of alloying elements on the phase diagrams of titanium alloys (schematic) [1]

The β stabilizing elements are divided into β isomorphous elements and β eutectoid elements, depending on the details of the resulting binary phase diagram. The two types of phase diagram are shown schematically in Fig. 10. The most frequently used β isomorphous elements in titanium alloys are V, Mo, and Nb. Sufficient concentrations of these elements make it possible to stabilize the β phase to room temperature. Other elements belonging to this group which are rarely used or not used at all because of density considerations, are Ta and Re. From the β eutectoid elements, Cr, Fe, and Si are used in many titanium alloys, whereas Ni, Cu, Mn, W, Pd, and Bi have only very limited usage. These elements are only used in one or two special purpose alloys [14]. Other β eutectoid forming elements, such as Co, Ag, Au, Pt, Be, Pb, and U, are not used at all in titanium alloys.

It should be mentioned that hydrogen belongs to these β eutectoid forming elements and that the low eutectoid temperature of 300°C in combination with the high diffusivity of hydrogen led to a special process of microstructure refinement, the so-called hydrogenation/dehydrogenation (HDH) process. HDH uses hydrogen as a temporary alloying element. Generally, the maximum hydrogen content in CP titanium and titanium alloys is strictly limited to about 125-150 ppm because of hydrogen embrittlement [14]. Two other elements that are often alloyed in titanium are tin and zirconium. These elements have extensive solid solubilities in the alpha and beta phases. Although they do not strongly promote phase stability, they retard the rates of transformation and are useful as strengthening agents. The effects and ranges of some alloying elements used in titanium are indicated in Table 3 [24].

Table 3. Ranges and effects of some alloying elements used in titanium

Alloying element	**Approximate range, wt %**	**Effect on structure**
Aluminum	2−7	Alpha stabilizer
Tin	2−6	Alpha stabilizer
Vanadium	2−20	Beta stabilizer
Molybdenum	2−20	Beta stabilizer
Chromium	2−12	Beta stabilizer
Copper	2−6	Beta stabilizer
Zirconium	2−8	Alpha and beta strengthener
Silicon	0.2−1	Improves creep resistance

e. β/α transformation

In the past years, most of the studies carried out on pure titanium concerning the Burgers orientation relationship involved the α to β transformation since the β phase cannot be retained at room temperature by slow cooling or quenching [25]. The transformation of the bcc β phase into the hexagonal α phase in CP titanium and titanium alloys can also occur martensitically or by a diffusion controlled nucleation and growth process depending on the cooling rate and alloy composition. The crystallographic orientation relationship between α and β was first studied for zirconium by Burgers and is therefore named the Burgers relationship:

$$(110)_\beta \parallel (0002)_\alpha$$

$$[1\bar{1}1]_\beta \parallel [11\bar{2}0]_\alpha$$

This relationship was confirmed later also for titanium [14,15]. According to this relationship, a bcc crystal can transform into 12 hexagonal variants, having different orientations with regard to the parent β crystal. The martensite transformation and the conventional nucleation and growth process both follow this relation [17].

1- Martensite transformation

The martensite transformation involves the movement of atoms by shear resulting in a microscopically homogeneous transformation of the bcc into the hcp crystal lattice over a given volume [14]. Unlike the martensite known in steels, which leads to strong distortion of the crystal lattice with an increase in hardness and strength, the hardening effect observed in titanium alloys for martensitic transformation is only moderate [15]. The transformed volume is usually plate shaped or better described geometrically as disk shaped for most titanium alloys. This hexagonal martensite is designated as α' and is observed in two morphologies: massive and “acicular” martensite. Massive martensite occurs only in pure titanium, very dilute alloys, and in alloys with a high martensitic transformation temperature. “Acicular” martensite occurs in alloys with higher solute content. The massive martensite consists of large irregular regions (size about 50-100 μm) without any clear internal features visible by light microscopy, but these regions contain packets of small, almost parallel α plates or laths (thickness about 0.5-1 μm). The “acicular” martensite consists of an intimate mixture of individual α plates, each of a different variant as shown in Fig. 11. Also, generally, the martensitic plates contain a high dislocation density and sometimes contain twins [14].

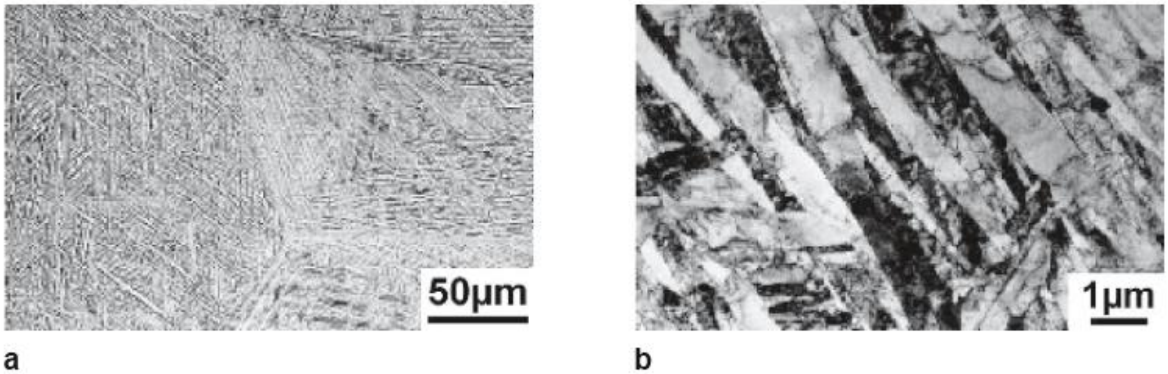

Fig. 11 “Acicular” martensite in Ti-6Al-4V quenched from the β phase field: (a) LM (b) TEM [14]

2- Nucleation and diffusional growth

When titanium alloys are cooled at sufficiently low rates from the β phase field into the (α+β) phase field, the α phase, which is incoherent with respect to the β phase, first nucleates preferentially at β grain boundaries leading to a more or less continuous α layer along β grain boundaries. During continued cooling α plates nucleate either at the interface of the continuous α layer or at the β grain boundary itself and grow into the β grain as parallel plates (a so-called α colony) [15]. They continue to grow into the β grain interior until they meet other α colonies nucleated at other grain boundary areas of the β grain [17]. The individual α plates are separated within the α colonies by the retained β matrix. These are commonly, but incorrectly, called β plates. The α and β plates are also often called α and β lamellae and the resulting microstructure is then designated as lamellar. An example of such a microstructure, which was obtained by slow cooling from the β phase field, is shown in Fig. 12 for the Ti-6Al-4V alloy. In such slowly cooled material, the size of the α colonies can be as large as half of the β grain size [14]. Also, grain growth is more than an order of magnitude faster when transformation takes place in the β phase field than when it occurs in the α field, at least at temperatures near the transus [24].

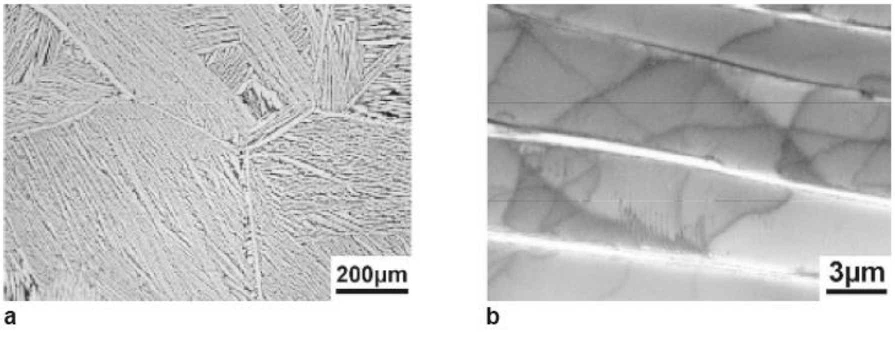

Fig. 12 Lamellar α+β microstructure in Ti-6Al-4V slowly cooled from the β phase field: (a) LM (b) TEM [1]

2. Alloy classification

Commercial titanium alloys are classified conventionally into three different categories (α, α+β, and β alloys) according to their position in a pseudo-binary section through a β isomorphous phase diagram, shown schematically in Fig. 13 A list of the most important commercial alloys belonging to each of these three different groups is shown in Table 4. In this table the common name, the nominal composition, and the nominal β transus temperature are stated for each alloy. [14]

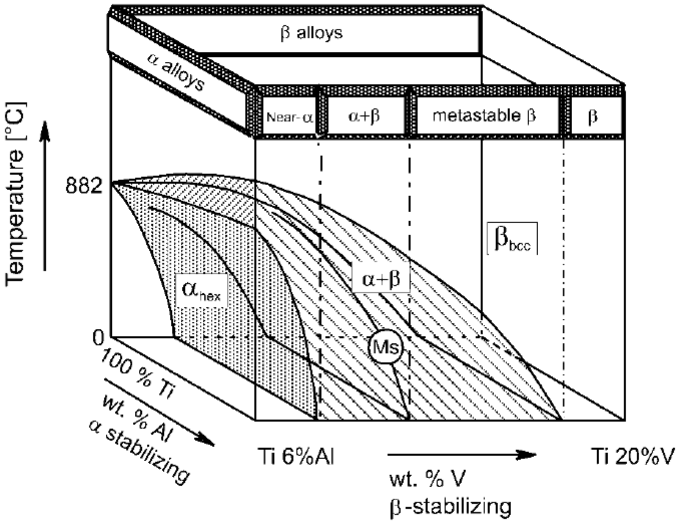

Fig. 13 Three-dimensional phase diagram to classify Ti alloys (schematically) [15]

Table 4. Important commercial titanium alloys [14]

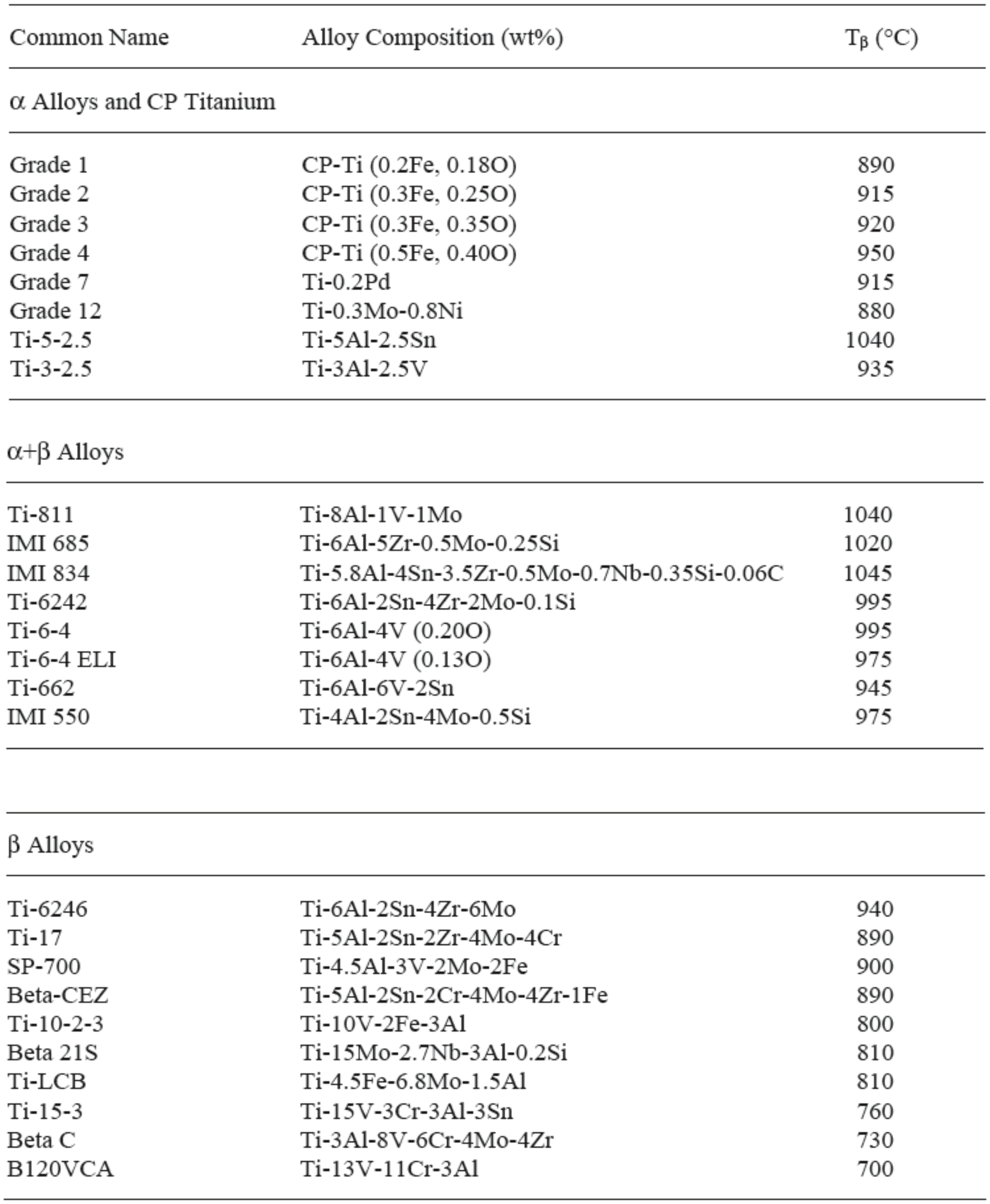

Common Name	Alloy Composition (wt%)	T_β (°C)
α Alloys and CP Titanium		
Grade 1	CP-Ti (0.2Fe, 0.18O)	890
Grade 2	CP-Ti (0.3Fe, 0.25O)	915
Grade 3	CP-Ti (0.3Fe, 0.35O)	920
Grade 4	CP-Ti (0.5Fe, 0.40O)	950
Grade 7	Ti-0.2Pd	915
Grade 12	Ti-0.3Mo-0.8Ni	880
Ti-5-2.5	Ti-5Al-2.5Sn	1040
Ti-3-2.5	Ti-3Al-2.5V	935
α+β Alloys		
Ti-811	Ti-8Al-1V-1Mo	1040
IMI 685	Ti-6Al-5Zr-0.5Mo-0.25Si	1020
IMI 834	Ti-5.8Al-4Sn-3.5Zr-0.5Mo-0.7Nb-0.35Si-0.06C	1045
Ti-6242	Ti-6Al-2Sn-4Zr-2Mo-0.1Si	995
Ti-6-4	Ti-6Al-4V (0.20O)	995
Ti-6-4 ELI	Ti-6Al-4V (0.13O)	975
Ti-662	Ti-6Al-6V-2Sn	945
IMI 550	Ti-4Al-2Sn-4Mo-0.5Si	975
β Alloys		
Ti-6246	Ti-6Al-2Sn-4Zr-6Mo	940
Ti-17	Ti-5Al-2Sn-2Zr-4Mo-4Cr	890
SP-700	Ti-4.5Al-3V-2Mo-2Fe	900
Beta-CEZ	Ti-5Al-2Sn-2Cr-4Mo-4Zr-1Fe	890
Ti-10-2-3	Ti-10V-2Fe-3Al	800
Beta 21S	Ti-15Mo-2.7Nb-3Al-0.2Si	810
Ti-LCB	Ti-4.5Fe-6.8Mo-1.5Al	810
Ti-15-3	Ti-15V-3Cr-3Al-3Sn	760
Beta C	Ti-3Al-8V-6Cr-4Mo-4Zr	730
B120VCA	Ti-13V-11Cr-3Al	700

a. α alloys

The group of α alloys in Table 4 consists of the various grades of CP titanium and α alloys which upon annealing well below the β transus contain only small amounts of β phase (2-5 vol%) stabilized by iron. The β phase is helpful in controlling the recrystallized α grain size and improves the hydrogen tolerance of these alloys. The four different grades of CP titanium differ with respect to their oxygen content from 0.18% (grade 1) to 0.40% (grade 4), this is added in order to increase the yield stress level. [14] The two alloys Ti-0.2Pd and Ti-0.3Mo-0.8Ni offer better corrosion resistance than CP titanium. Their common names are grade 7 and grade 12, respectively, and the iron and oxygen limits are identical to grade 2 of CP titanium. [14] These alloys are primarily used in the chemical and process engineering industries. Here excellent corrosion behavior and deformability are of prime concern while high (specific) strength only ranks second. The various commercially pure CP titanium grades differ primarily in oxygen content [15].

b. α + β Alloys

Among the α + β alloys, Ti-6Al-4V is by far the most popular titanium alloy. More than 50% of all alloys in use today are of this composition. The alloy was developed in the early 1950s in the United States at the Illinois Institute of Technology and is therefore one of the very first titanium alloys to be made. Two reasons for the success of Ti-6Al-4V are first the good balance between its various mechanical properties and second it is by far the most intensively tested titanium alloy. These are major advantages, especially in the aerospace industry, which is the largest user of Ti-6Al-4V [15].

c. β Alloys

All the alloys in β alloy group in Table 4 are actually metastable β alloys because they all are located in the equilibrium (α + β) phase region of the phase diagram [14]. Over the last few decades the importance of metastable alloys has steadily increased. These alloys can be hardened to extremely high strength levels of more than 1400 MPa. The complex microstructure enables the designer to optimize for both high strength and high toughness. This is true for TIMETAL 10-2-3 and Beta C. Other alloys like TIMETAL 15-3 can be deformed at room temperature down to thin foils. In particular, TIMETAL 21S was specially developed as an oxidation resistant foil alloy to be used as the matrix for long fiber reinforced titanium alloys. The widespread application of these alloys is, however, limited by their relatively high specific weight, modest weldability, poor oxidation behavior, and complex microstructure [24]

3. Mechanical properties

From the four different hardening mechanisms in metallic materials (solid solution hardening, strengthening by a high dislocation density, boundary hardening, and precipitation hardening) solid solution and precipitation hardening are present in all commercial titanium alloys and should be discussed separately for the α phase and for the β phase [14]. Boundary hardening plays a significant role in the α+β alloys cooled at high rates from the β phase field. This reduces the α colony size to a few α plates or causes a martensitic transformation. In both cases, a high dislocation density is created, which also contributes to the hardening [24].

1- Hardening of the Alpha Phase

The α phase is significantly hardened by the interstitial element oxygen. This can best be seen by comparing the yield stress values of the CP titanium grades 1-4 with oxygen levels between 0.18 and 0.40%. By this increase in oxygen content, the yield stress is increased from 170 MPa (grade 1) to 480 MPa (grade 4). In commercial titanium alloys the oxygen content varies between about 0.08% and 0.20% depending on alloy type. Substitutional solid solution hardening of the α phase is caused mainly by the elements Al, Sn, and Zr, which have fairly large atomic size differences to titanium and also large solid solubilities in the α phase [14].

2- Hardening of the Beta Phase

It is difficult to analyze solid solution strengthening of the β phase in a traditional sense because in fast cooled metastable β alloys, the precursors of the metastable ω and β' phases cannot be separated from the solute effects. Also, in fully aged microstructures, it is difficult to separate the hardening due to α precipitates from the solute effects. In this case, an important solid solution strengthening effect of the β phase is due to the alloy element partitioning that accompanies α precipitation [14].

4. The Microstructure of Titanium Alloys

The microstructure of conventional titanium alloys is primarily described in terms of the size and arrangement of the two phases, α and β. The two extreme cases of phase arrangements are the lamellar microstructure, which is generated upon cooling from the β phase field as mentioned earlier and the equiaxed microstructure, which is a result of a recrystallization process. Both types of microstructure can have a fine as well as a coarse arrangement of their two phases. The influence of the various microstructures on the mechanical behavior of titanium alloys has been the subject of numerous investigations. Table 5 shows qualitatively how the sizes of the phases (comparison of fine and coarse microstructures) on the one hand, and the arrangement of the phases (comparison between lamellar and equiaxed microstructures) on the other, have an effect on some important selected mechanical properties [15].

Table 5. Influence of microstructure on selected properties of titanium alloys [15]

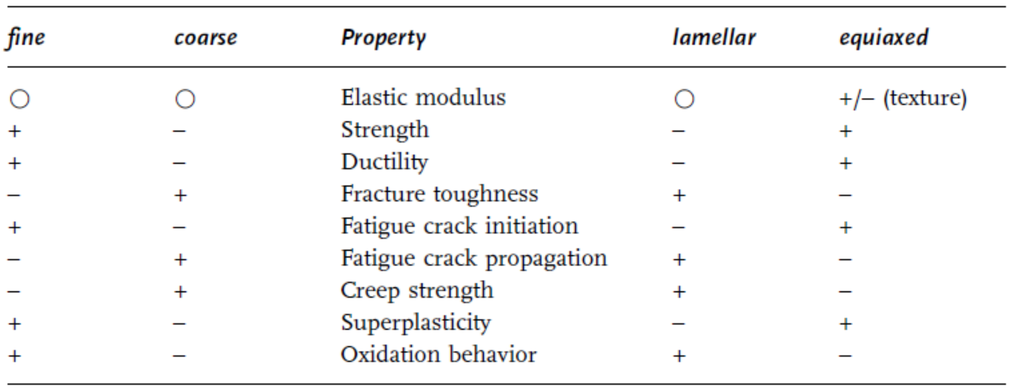

fine	*coarse*	*Property*	*lamellar*	*equiaxed*
○	○	Elastic modulus	○	+/– (texture)
+	–	Strength	–	+
+	–	Ductility	–	+
–	+	Fracture toughness	+	–
+	–	Fatigue crack initiation	–	+
–	+	Fatigue crack propagation	+	–
–	+	Creep strength	+	–
+	–	Superplasticity	–	+
+	–	Oxidation behavior	+	–

Generally, the different microstructures are generated by different thermomechanical treatments. These are considered as a complex sequence of solution heat treatment, deformation, recrystallization, aging, and annealing for stress relief as schematically outlined in Fig. 14 [15].

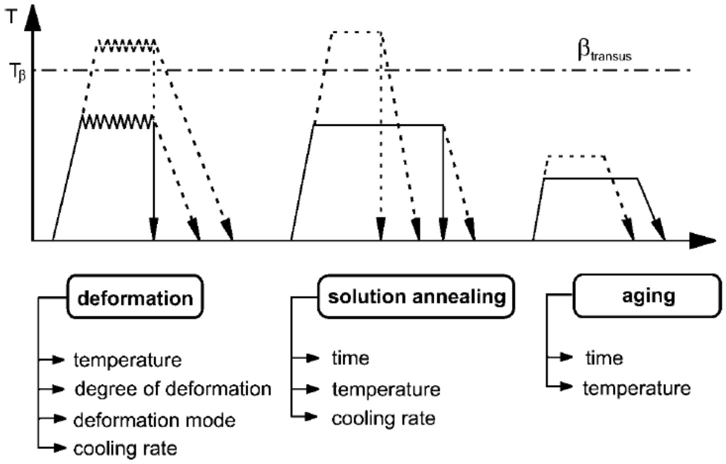

Fig. 14 Thermomechanical treatment of titanium alloys [2]

An important point for thermomechanical treatment is the β-transus temperature, which separates the single phase β field from the two-phase α+β field. Lamellar microstructures are a result of simple cooling from temperatures above the β-transus temperature. Once the temperature falls below the β-transus, α nucleates at grain boundaries and then grows as lamellae into the (prior) β grain. An example of this structure is shown for the Ti-6Al-4V alloy in a high temperature microscopy sequence in Fig. 15.

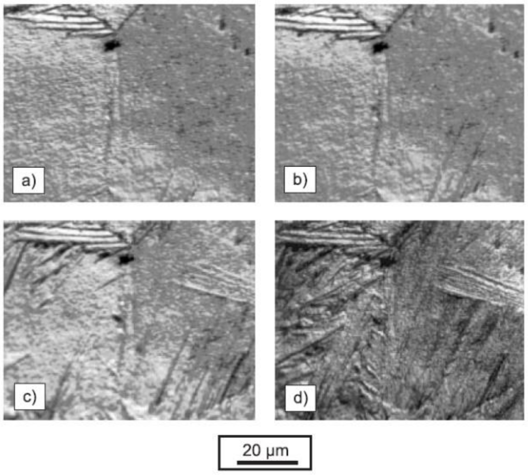

Fig. 15 a) → d) shows how α nucleates at grain boundaries and then grows as lamellae into the prior β grain when cooling from the β-transus field of Ti-6Al-4V (high-temperature microscopy) [2]

Depending on the cooling rate, the lamellae are either fine or coarse. Slow cooling from the phase field results in pure lamellar microstructures shown in Fig. 16-a, with the lamellae becoming coarser with reduced cooling rate. Rapid quenching leads to the martensitic transformation of β, resulting in a very fine needle-like microstructure. The chemical compositions of the α and β phases change in the two-phase field with decreasing temperature under equilibrium conditions. The metallographic figures of all slowly cooled specimens show β as a small seam around the coarse and light colored α lamellae, as clearly shown in Figs. 16-a, c, d. With high cooling rates from temperatures above the martensitic start temperature and through the two-phase field, β transforms into martensite (Fig. 16-d). [15]

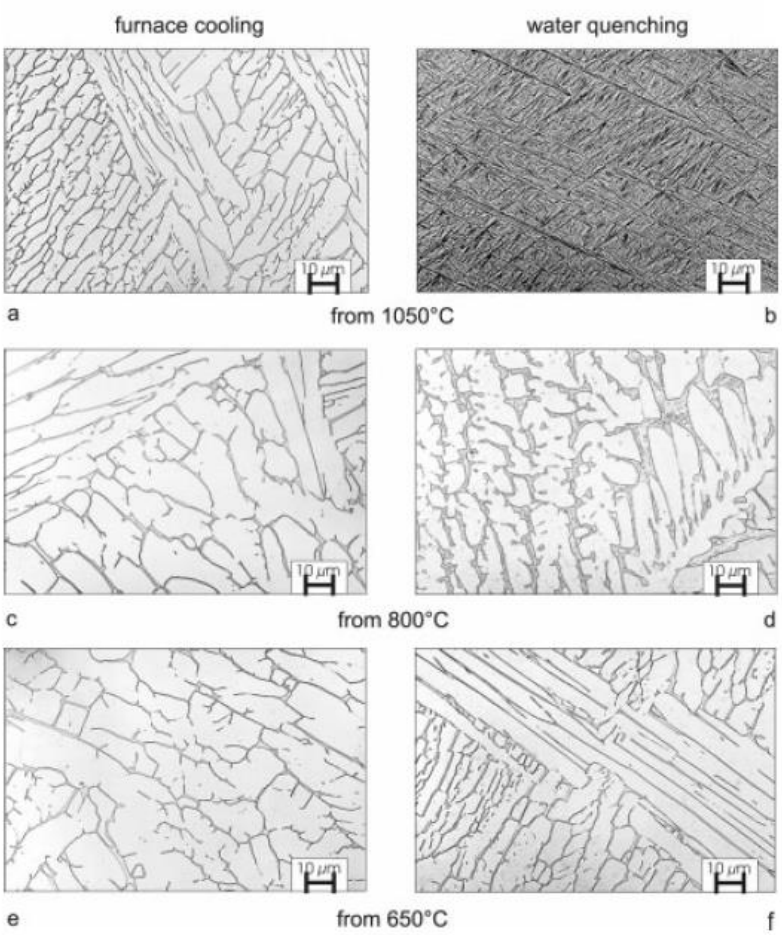

Fig. 16 Microstructure of Ti-6Al-4V after slow cooling (50 C/h) from a) → c) → e), and water quenching from 1050C in b), 800C in d), and 650C in f). [2]

The martensitic start temperature varies depending on the starting structure and the homogeneity of the microstructure. At lower temperatures, the β volume fraction further decreases and no longer transforms to martensite at temperatures below the martensitic start temperature, as shown in Fig. 16-f. [15]

Unlike lamellar microstructures, equiaxed microstructures are the result of a recrystallization process. [15] Therefore, the alloy first has to be highly deformed in the α+β field to introduce enough cold work into the material. Upon solution heat treatment at temperatures in the two-phase field, recrystallized and equiaxed microstructures are generated, as seen in Fig. 17-a. Extended annealing coarsens the equiaxed microstructure (Fig. 17-b). Solution heat treatment just below the β-transus temperature results in bimodal microstructures that can be considered to be a combination of lamellar and equiaxed microstructure. [15]

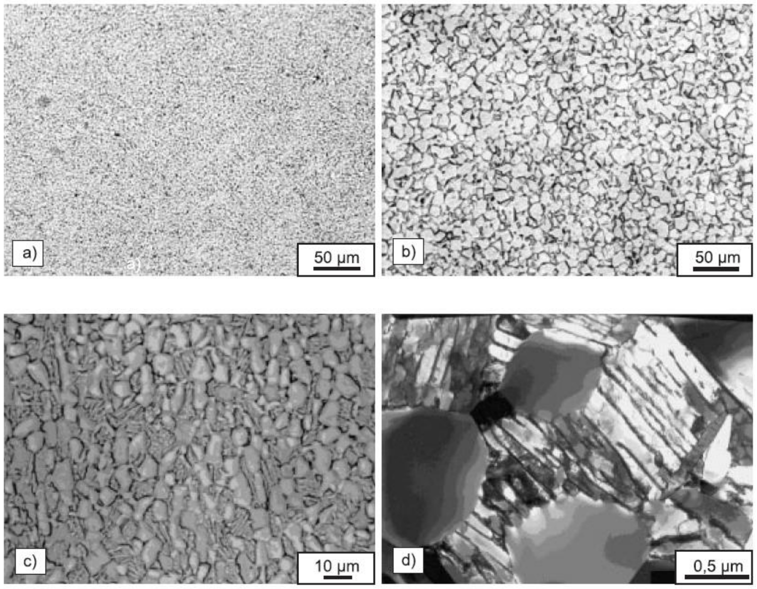

Fig. 17 Equiaxed microstructures of Ti-6Al-4V via recrystallization: a) fine equiaxed; b) coarse equiaxed; c, d) bimodal (OM, TEM). [2]

Finally, the various microstructures have a strong influence on the mechanical behavior of titanium alloys. Fine-scale microstructures increase the strength as well as the ductility. Furthermore, they retard crack nucleation and are a prerequisite for superplastic deformation. Coarse microstructures, on the other hand, are more resistant to creep and fatigue crack growth. Equiaxed microstructures often have high ductility as well as fatigue strength and are preferred for superplastic deformation, while lamellar structures have high fracture toughness and show superior resistance to creep and fatigue crack growth. Since bimodal microstructures combine the advantages of lamellar and equiaxed structures, they exhibit a well-balanced property profile. [15]

a. Metallographic Preparation of the Microstructure

In the metallography of titanium, time, resources, and the need for investigation are important considerations [26-28] Metallographic preparation is very important and of great interest because the mechanical properties of titanium alloys are determined primarily by the chemical composition and the microstructure. [15] Unlike steel, the metallography of titanium and its alloys is more difficult, especially for pure titanium where smearing and scratches can be quite difficult to eliminate. [27] The high ductility of titanium is the main reason why it is difficult to cut, grind and polish and hence a problem for microscopic observation. [28] The cutting, for example, of titanium specimens should always be done with water cooling to prevent the local overheating that is caused by its low thermal conductivity in comparison to other metals. Furthermore, the velocity of the cutting blade and the feed rate should be reduced. Titanium tends to create deformed surface layers, which may exhibit pseudo microstructures. [15]

One sophisticated solution to this problem is electrolytic polishing. However, this is only recommended for polishing very pure titanium, which is otherwise extremely difficult to polish mechanically. [15] The final polishing will in general be repeated in short steps several times, followed by etching and verification of the microstructure under the optical microscope. A universal etchant is a solution, consisting of 3 ml HF (40% conc.) and 5 ml HNO_3 (65% conc.) in

100 ml H_2O. Images of very fine precipitates or transformation products in Ti-alloys can only be obtained with the aid of a transmission electron microscope. Special preparation is necessary for the thin foil specimens required here [26].

5. Dynamic transformation in titanium

Dynamic transformation was first discovered in steel by Yada and co-workers in the late 1980s. They showed that austenite can be transformed into ferrite by deformation at temperatures above the Ae_3. [4-6] Recently, various researchers around the world have proposed explanations of this phenomenon. The deformation behavior of commercially pure titanium during cold and hot working was previously studied by many researchers [8]. Koike and co-workers [16] studied the deformation behavior of Ti-5.5 wt%Al-1.5 wt%Fe alloy and produced an increase in the β volume fraction by deforming at temperatures below the β-transus. Dynamic transformation was also observed in the work of Xu and Zhu [1], where distinct amounts of softening were observed when their CP titanium grade 2 was deformed below the β-transus.

However, there was no thermodynamic explanation for this phenomenon at that time. Jonas et al. [9] recently explained the softening mechanism in a near-alpha Ti alloy (IMI-834).

1. Energy barriers

The mechanical activation concept was introduced in steels. The mechanical activation by softening is described by the driving force which is the difference between the critical stress of the hard phase – the yield stress of the soft phase. On the other hand the energy barriers which are represented by delta free energy between autenite and ferrite, the shear of accommodation and the shear of dilatation. For dynamic transformation to exist the driving force must overcome the energy barriers. If the driving force is not big enough to overcome the energy barriers then dynamic transformation won't happen. Dynamic transformation is also observed in titanium and titanium alloys but here the harder phase is the room temperature HCP alpha phase so here we deform at temperatures below the beta transus where the softer phase beta phase is formed. So basically in steels the transformation temperature is increased after deformation while in titanium the transformation temperature is decreased [8].

2. Softening in titanium alloys

Transformation softening was observed in different titanium and titnaium alloys. Though it was not the main area of interest. Transformation softening was observed in the work done by Xu and Zhu [1] where they deformed commercially pure titanium at different temperature and different strain rates. If you can notice, at 900 C, softening below the yield stress is observed at different strain rates. In their paper, the authors concluded that these abnormally low flow stresses were attributable to dynamic recrystallization. However, it is not possible for dynamic recrystallization, which acts to remove dislocations by grain boundary migration (discontinuous dynamic recrystallization) or by annihilation and rearrangement (continuous dynamic recrystallization) to reduce the flow stress to below the level of the yield stress without a phase change. Similar remarks apply to the work hardening mechanism of dynamic recovery, which also involves the rearrangement of dislocations. This cannot produce negative work hardening and therefore cannot reduce the flow stress to values below the yield stress [8].

3. Scope and Objectives

Transformation softening in commercially pure titanium was first observed by Xu et al. [1]. The objective of this study was to investigate the occurrence of dynamic transformation (DT) in commercially pure titanium grade 2. This was done by performing hot compression tests at temperatures below the β-transus and examining the microstructural changes. The driving forces and obstacle energies associated with the DT of α-Ti have also been considered. The volume fractions of the β phase produced by dynamic transformation have been measured as well. Finally, the minimum temperature at which DT can take place has been determined.

4. Experimental Procedure

1. Commercially pure titanium

A commercially pure titanium grade 2 (β-transus = 915 ^{o}C) was obtained from the McMaster Co. with the composition shown in Table 6. Cylindrical specimens 9 mm in height and 6 mm in diameter were machined from cylindrical rods.

Table 6 Chemical composition (mass %) of CP Ti grade 2

Fe	C	H	O	N	Ti
≤0.30	≤0.10	≤0.015	≤0.25	≤0.03	Bal.

2. Heat treatment

Samples were annealed at 800 ^{o}C for 1 h to homogenize the microstructure and remove any residual stresses [21,29]. A box furnace with an argon gas atmosphere was employed. Samples were finally air cooled to room temperature. Stainless steel envelopes were used to protect the samples from oxidation. With the aid of this procedure, an equiaxed microstructure was produced with an average grain size of 40 um. These results are similar to those reported in references [17,19,21]. This annealing process is illustrated schematically in Fig. 18.

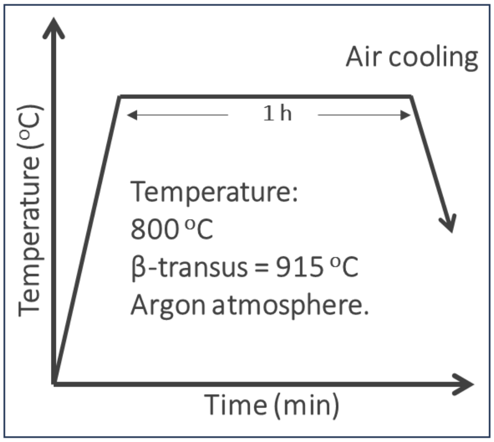

Fig. 18 Annealing schedule of the machined CP Ti samples

3. Compression deformation tests

Hot compression tests were carried out on an MTS 100 kN machine, Fig. 19. The experiments were conducted at elevated temperatures using a radiant heating furnace under an argon protective atmosphere. The temperatures were measured using a thermocouple in contact with the sample.

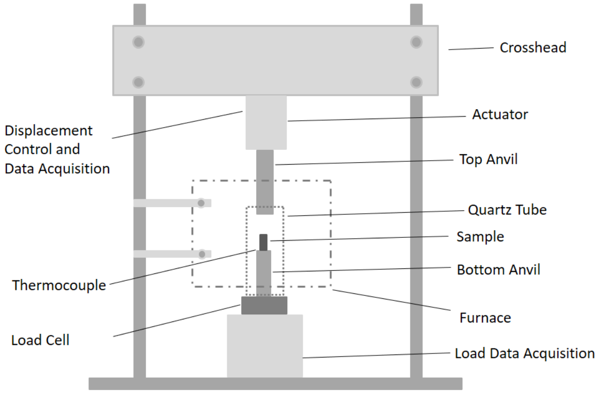

Fig. 19 Schematic of the 100kN MTS compression machine.

Deformation temperatures between 750 and 900 ^{o}C were used to study the effect of deformation below the b-transus. Tests between 930 and 970 ^{o}C were also carried out to determine the critical stress required to form the fresh beta phase at temperatures above the β-transus. To reduce the amount of oxygen absorbtion [14], a 5 C/s heating rate was used to reduce the absorbtion time. Samples were held at temperature for 2 min to ensure a homogenous temperature distribution throughout the specimen.

A schematic view of the MTS compression machine is presented in Fig. 20. Samples were deformed to a strain of 0.8 at a strain rate of 0.01 s-1. These were then water quenched to freeze the phases formed at each temperature. The deformation process is described schematically in Fig. 20.

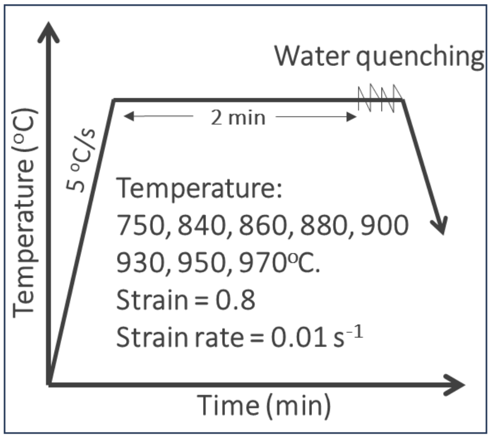

Fig. 20 Thermomechanical schedule of the compression tests

4. Microstructural characterization

The deformed samples were investigated using optical microscopy. They were sectioned along their transverse axes and hand ground using silicon carbide papers with particle sizes of 320, 400, 600, and 800 mesh. Samples were polished using 3um and 1um diamond suspensions and finally etched for 10 s with a solution of 10 mL HF + 5 mL HNO_3 + 85 mL H_2O.

5. *Experimental Results*

6. **Flow stress**

Stress-strain curves were generated from the hot compression tests at different temperatures leading to the flow curves shown in Fig. 21.

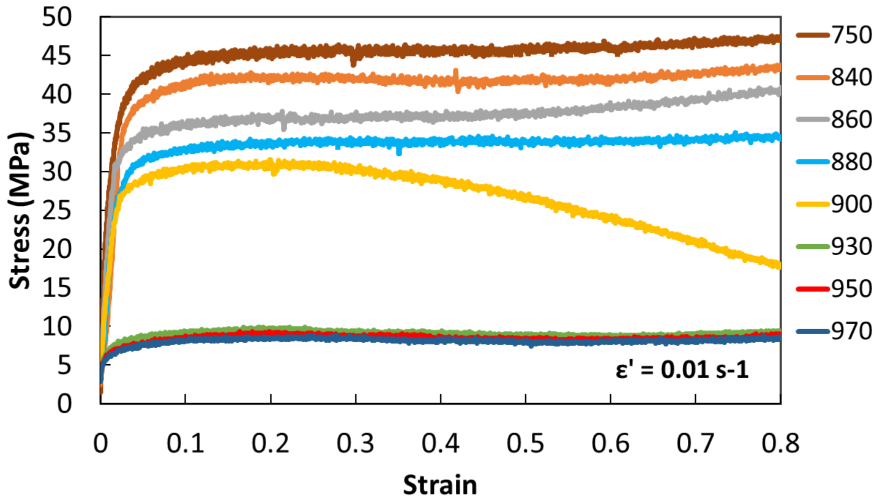

Fig. 21 Stress-strain curves determined at eight different temperatures

Three of the temperatures were in the beta phase region and five below the β-transus. At 900 ^{o}C (15 ^{o}C below the β-transus), there is considerable flow softening. At this temperature, the driving force is high enough to convert 50% of the harder alpha phase into the softer beta phase. Such flow softening has also been observed by other authors, although this has generally been attributed to DRX or texture softening [2].

7. **Microstructure**

Microstructural evidence is presented to support the view that dynamic transformation takes place and that the β phase forms at temperatures below the β-transus. When the phase fractions were measured, no beta phase was observed in the as-received material nor when it was deformed at 750 ^{o}C (Fig. 22-a,b).

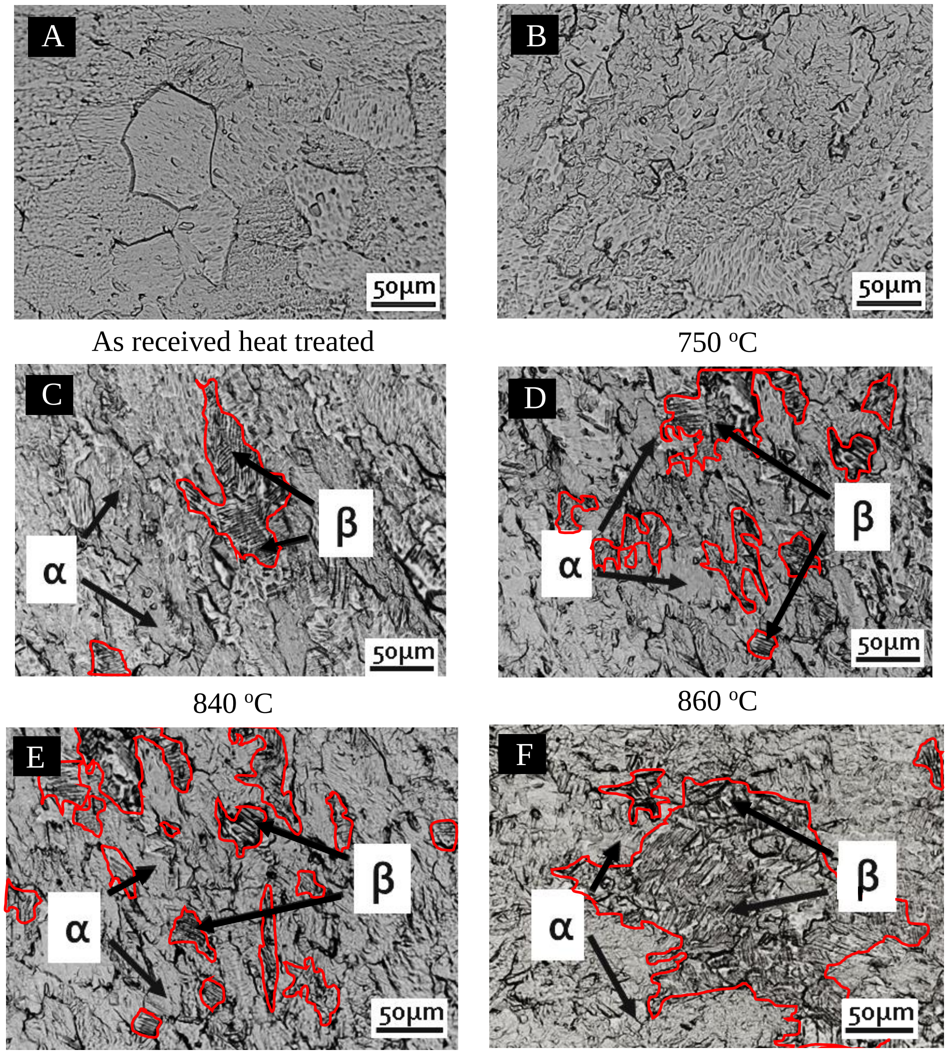

As received heat treated

750 °C

840 °C

860 °C

880 °C

900 °C

Fig. 22. Optical micrographs show an increase in β-phase formation with increasing deformation temperature.

Hexagonal martensite, as mentioned in Chapter 2, is designated here as α' and is referred to as massive martensite as observed in pure titanium. The massive martensite consists of large irregular regions (size about 50-100 μm) without any clear internal features. As seen in Fig. 22, these regions contain packets of small, almost parallel α plates or laths (thickness about 0.5-1 μm). Rapid quenching from the deformation temperature leads to the martensitic formation of β, resulting in the very fine needle-like microstructure seen in Fig. 22-C-F.

Beta phase (α') formation begins at 840 ºC and achieves a level of 30% β as seen in Fig. 22-C. Some beta martensite fractions are also observed and the amount of the phase increases with the deformation temperature. More than 50% beta martensite is formed at 900 ºC.

The beta volume fraction formed at different temperatures is highlighted in red in Fig. 5. The areas highlighted representing beta martensite were measured using the Image J software using a standard deviation of 5%. This is plotted against formation temperature in Fig. 23.

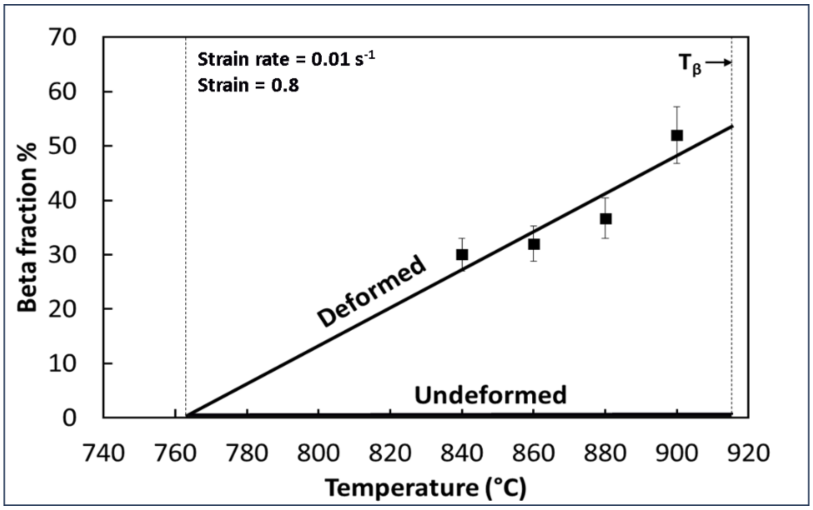

Fig. 23 Comparison of the beta phase fractions in the undeformed and deformed samples.

8. Driving force

The driving force for the transformation was calculated from the difference between the critical stress of the harder alpha phase and the yield stress of the softer fresh beta phase as seen in Fig. 24.

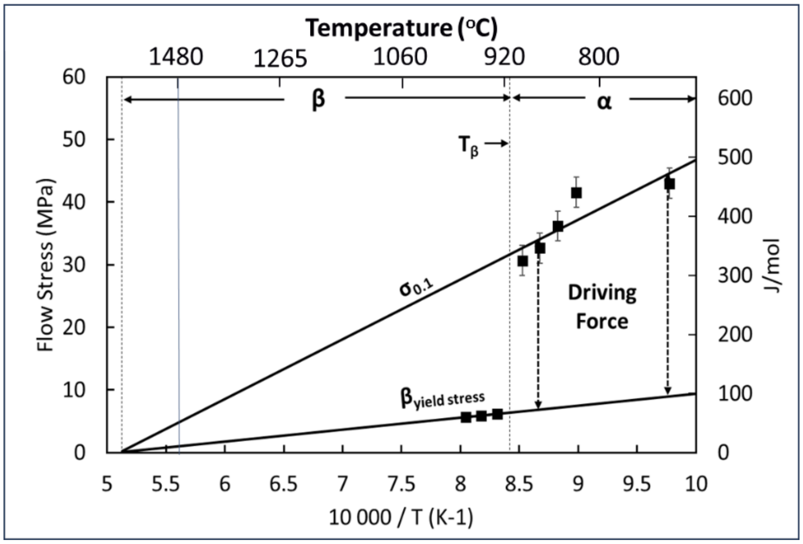

Fig. 24 The $\boldsymbol{\sigma}$ ($\boldsymbol{critical–hard\ phase}$) – $\boldsymbol{\sigma}$ ($\boldsymbol{yield–soft\ phase}$) for the α → β transformation

This force is compared with the driving force for transformation proposed in reference [8], see Fig. 25. At 880 ^{o}C, the driving force of 288 J/mol is greater than the barrier energy of 65 J/mol. On the other hand, at 750 ^{o}C, the driving force of 378 J/mol is lower than the 565 J/mol obstacle energy that corresponds to this temperature [8].

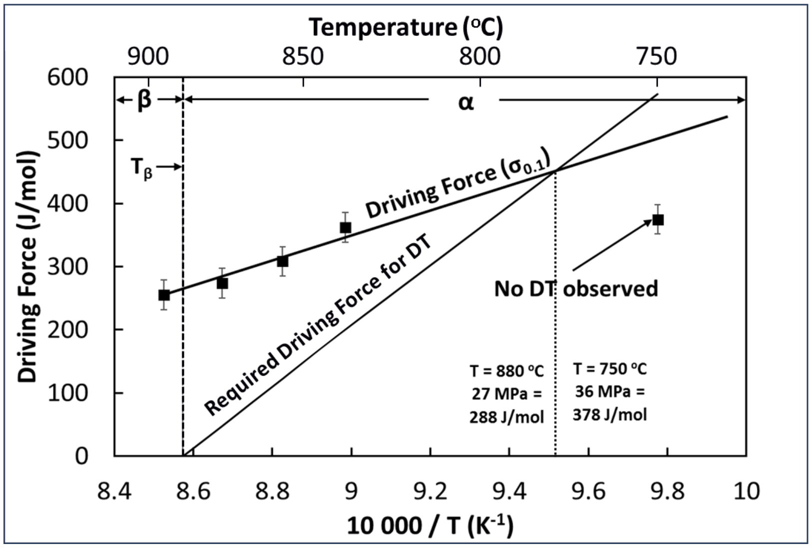

Fig. 25 The driving force for the α → β transformation

9. The minimum temperature to induce transformation

Finally, the minimum temperature at which transformation can be induced was calculated from the peak stress and the critical stress calculated from the literature, see Fig. 26. The peak stress is employed here because it is an estimate of the stress required to initiate transformation into the beta phase.

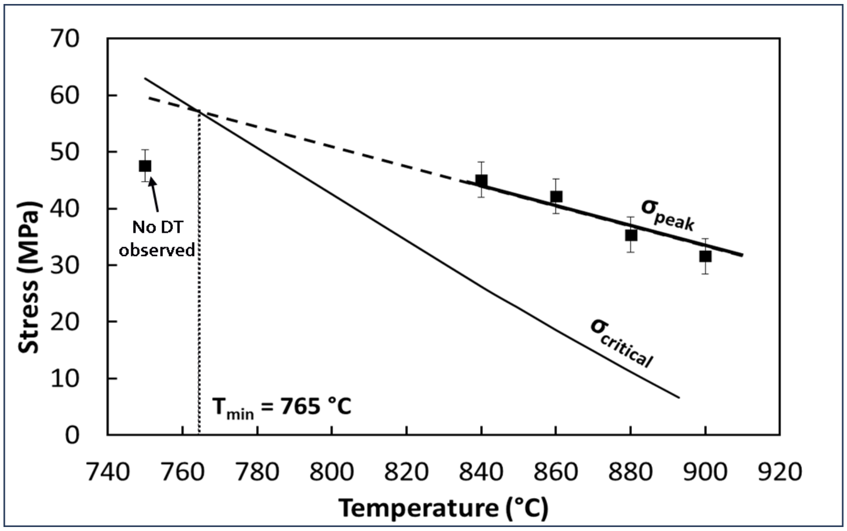

Fig. 26 The minimum temperature to induce DT in CP Tfi Grade 2.

6. Conclusion

Hot compression tests were carried out on commercially pure titanium grade 2. Dynamic transformation was observed to take place leading to the following conclusions:

- Dynamic transformation takes place in commercially pure titanium grade 2 when it is deformed at temperatures below the β transus.
- The driving force for the transformation is the flow stress difference between the work hardened α at the critical stress and the yield stress of the fresh β phase that takes its place. These driving forces fall in the range 200–500 J/mol.
- The obstacles to the transformation consist of the free energy difference between the two phases and the work of dilatation, both of which depend on temperature.
- At temperatures of 840, 860, 880, and 900 ^{o}C, the β volume fraction increases by 30, 32, 36, and 55%, respectively.
- The minimum temperature at which dynamic transformation can be induced in CP Ti Grade 2 is 765 ^{o}C. No dynamic transformation was observed below this temperature.

7. Future Work

In the future work, the extent to how dynamic transformation in commercially pure titanium is applied is to be studied in depth and the main focus will be on:

- Methods of calculating the critical strain and energy barriers have been developed for steel. The extent to which these approaches apply to titanium and titanium alloys will be assessed.
- Employing different strains and strain rates to deeply understand the behavior of commercially pure titanium at different temperatures.
- Perform EBSD examinations to determine the microstructural features of the transformation.
- Determination of the kinetics of transformation and recrystallization is to be studied and implemented in future work.

8. References

1- Xu, C., & Zhu, W. (2010). Transformation mechanism and mechanical properties of commercially pure titanium. Transactions of Nonferrous Metals Society of China, 20(11), 2162-2167.

2- CHEN Yong-hong. Elementary analysis of the current situation of the titanium industry in U.S.A., Japan and China [J]. Titanium Industry Progress, 2005, 22(4): 12−14. (in Chinese)

3- WU Quan-xing. Present situation and prospect of Ti mill products in Japan [J]. Rare Metals Letters, 2004, 23(1): 11−14. (in Chinese)

4- H. Yada, Y. Matsumura, T. Senuma, Massive type transformation induced by hot deformation in low carbon steels, Proceedings of the International Conference on Martensitic Transformation, JIM 1986, pp. 515–520.

5- H. Yada, Y. Matsumura, T. Senuma, A new thermomechanical heat treatment for grain refining in low carbon steels, Proceedings of the 1st Conference on Physical Metallurgy of Thermomechanical Processing of Steels and Other Metals, ISIJ (THERMEC-88) 1988, pp. 200–207.

6- H. Yada, C.M. Li, H. Yamagata, Dynamic γ-N α transformation during hot deformation in iron–nickel–carbon alloys, ISIJ Int. 40 (2000) 200–206.

7- Aranas Jr, C., Jonas, J.J. (2015). Effect of Mn and Si on the dynamic transformation of austenite above the Ae3 temperature, Acta Materialia, 82.

8- Aranas, C., Foul, A., Guo, B., Fall, A., Jahazi, M., & Jonas, J. J. (2017). Determination of the critical stress for the initiation of dynamic transformation in commercially pure titanium. Scripta Materialia, 133, 83-85.

9- Jonas, J. J., Aranas Jr, C., Fall, A., & Jahazi, M. (2017). Transformation softening in three titanium alloys. Materials & Design, 113, 305-310.

10- Koike, J., Shimoyama, Y., Ohnuma, I., Okamura, T., Kainuma, R., Ishida, K., & Maruyama, K. (2000). Stress-induced phase transformation during superplastic deformation in two-phase Ti–Al–Fe alloy. Acta Materialia, 48(9), 2059-2069.

11- Yang, H. S., Gurewitz, G., & Mukherjee, A. K. (1991). Mechanical Behavior and Microstructural Evolution during Superplastic Deformation of Ti–6Al–4V. Materials Transactions, JIM, 32(5), 465-472.

12- Zong, Y. Y., Shan, D. B., Xu, M., & Lv, Y. (2009). Flow softening and microstructural evolution of TC11 titanium alloy during hot deformation. Journal of Materials Processing Technology, 209(4), 1988-1994.

13- Poliak, E. I., & Jonas, J. J. (1996). A one-parameter approach to determining the critical conditions for the initiation of dynamic recrystallization. Acta Materialia, 44(1), 127-136.

14- Lütjering, G., and Williams, J. C. (2007). Titanium. Materials engineer and processes. Springer, 2 edition.

15- Leyens, C., Peters, M., John, W., Sons, & Wiley, I. (2003). Titanium and titanium alloys: fundamentals and applications.

16- Szkliniarz, W., & Smołka, G. (1995). Analysis of volume effects of phase transformation in titanium alloys. Journal of Materials Processing Technology, 53(1), 413-422.

17- Shinbine, A., Garcin, T., & Sinclair, C. (2016). In-situ laser ultrasonic measurement of the hcp to bcc transformation in commercially pure titanium. Materials Characterization, 117, 57-64.

18- Gurao, N. P., Kapoor, R., & Suwas, S. (2011). Deformation behaviour of commercially pure titanium at extreme strain rates. Acta Materialia, 59(9), 3431-3446.

19- Nemat-Nasser, S., Guo, W. G., & Cheng, J. Y. (1999). Mechanical properties and deformation mechanisms of a commercially pure titanium. Acta Materialia, 47(13), 3705-3720.

20- Froes, F. H. (2015). Titanium : physical metallurgy, processing, and applications.

21- Zeng, Z., Zhang, Y., & Jonsson, S. (2009). Deformation behaviour of commercially pure titanium during simple hot compression. Materials & Design, 30(8), 3105-3111.

22- Ahmed, M., Wexler, D., Casillas, G., Savvakin, D. G., & Pereloma, E. V. (2016). Strain rate dependence of deformation-induced transformation and twinning in a metastable titanium alloy. Acta Materialia, 104, 190-200.

23- Huang, X., Suzuki, K., Yuasa, M., & Chino, Y. (2014). Microstructural and textural evolution of pure titanium during differential speed rolling and subsequent annealing. Journal of Materials Science, 49(8), 3166-3176.

24- Donachie, M. J. (2000). Titanium : a technical guide.

25- Seward, G. G. E., Celotto, S., Prior, D. J., Wheeler, J., & Pond, R. C. (2004). In situ SEM-EBSD observations of the hcp to bcc phase transformation in commercially pure titanium. Acta Materialia, 52(4), 821-832.

26- Luther M. Gammon, R. D. B., John M. Packard, Kurt W. Batson, Rodney Boyer, and Charles W. Domby,, & Company, T. B. (2004). Metallography and Microstructures of Titanium and Its Alloys. ASM Handbook, Volume 9.

27- Voort, G. V. (2015). Metallographic Preparation of Titanium and its Alloys. Buehler Tech-Notes, 3(3).

28- Taylor, B., & Weidmann, E. (2016). Metallographic preparation of titanium. Struers ApS.

29- Hajizadeh, K., Eghbali, B., Topolski, K., & Kurzydlowski, K. J. (2014). Ultra-fine grained bulk CP-Ti processed by multi-pass ECAP at warm deformation region. Materials Chemistry and Physics, 143(3), 1032-1038.

Appendix

A- Manuscript submitted to the journal Materials Science and Engineering A

Elsevier Editorial System(tm) for Materials Manuscript Draft

Title: Dynamic transformation of $\alpha \rightarrow \beta$ titanium at temperatures below the β-transus in commercially pure titanium

Article Type: Short Communication

Keywords: dynamic transformation, net softening, commercially pure titanium

Corresponding Author: Anes Foul

Corresponding Author's Institution: McGill University First Author: Anes Foul

Order of Authors: Anes Foul; Clodualdo Aranas Jr; Baoqi Guo; John J. Jonas

Abstract: Hot compression tests were carried out on commercially pure titanium grade 2 at temperatures below the β-transus (915 °C). At temperatures of 840, 860, 880, and 900 °C, the β volume fraction increased by 30, 32, 36, and 55%, respectively. The minimum temperature at which dynamic transformation could be induced was 765 °C. The driving force for transformation given by the net softening associated with the formation of the lower flow stress beta phase was calculated to fall in the range 200-500 J/mol.

*Prime Novelty Statement

Prime Novelty Statement

1- Dynamic transformation is shown to take place in commercially pure titanium grade 2.
2- Hot compression flow curves and microstructural observations are presented for Ti grade 2 deformed over the temperature range 750 to 970 °C.
3- The beta volume fractions are calculated as well as the minimum temperature at which dynamic transformation can be induced together with the driving force for transformation.

*Manuscript

Dynamic transformation of α → β titanium at temperatures below the β-transus in commercially pure titanium

Anes Foul[1], Clodualdo Aranas Jr.[1], Baoqi Guo[1], John J. Jonas[1]

[1]Materials Engineering, McGill University

3610 University St., Montreal, Canada H3A 0C5

Abstract

Hot compression tests were carried out on commercially pure titanium grade 2 at temperatures below the β-transus (915 ^{o}C). At temperatures of 840, 860, 880, and 900 ^{o}C, the β volume fraction increased by 30, 32, 36, and 55%, respectively. The minimum temperature at which dynamic transformation could be induced was 765 ^{o}C. The driving force for transformation given by the net softening associated with the formation of the lower flow stress beta phase was calculated to fall in the range between 200-500 J/mol.

Keywords: dynamic transformation, net softening, commercially pure titanium

Introduction

The dynamic transformation of titanium has been reported to take place when it is deformed at temperatures below the β-transus; under these conditions the harder α phase transforms into the softer β phase. Koike and co-workers [1] observed that the beta volume fraction increases significantly when samples of Ti- 5.5 wt%Al-1 wt%Fe were strained in tension at temperatures in the range 777 °C to 927 °C. Evidence of dynamic transformation in commercially pure titanium was also observed by Xu and co-workers [2]. Sub-transus softening was obtained when CP Ti grade

2 was deformed at temperatures below the β-transus (915 ^{o}C). They attributed the softening to dynamic recrystallization (DRX) even though flow stresses below the yield stress were produced. This softening was later explained as resulting from dynamic transformation where there is a displacive phase change from α to the softer β [3]. Evidence for dynamic transformation has also been reported in other titanium alloys [4,5].

Recently, Aranas and co-workers [6] presented a thermodynamic explanation for dynamic transformation in pure titanium where the driving force for transformation is given by the difference between the critical stress of the deformed α phase at the initiation of transformation and the yield stress of the newly formed β phase that takes its place. In steels, the critical stress is determined using double differentiation [7]. In titanium, on the other hand, this method is not applicable due to the high initial work hardening rate. Here the critical stress is calculated by equating the driving force with the total obstacle energy. The energy barriers consist of the free energy difference between β and α and the work of dilatation associated with the transformation. The work of shear accommodation is considered negligible during transformation [6].

In the current work, hot compression tests were carried out on commercially pure titanium grade 2 in a 100 kN MTS machine at temperatures between 750 and 970 ^{o}C. Samples were deformed to a true strain of 0.8 at a strain rate of 0.01 s-1. Under these conditions, there is considerable sub-transus softening accompanied by an increase in the β volume fraction. The β volume fraction has been observed to increase to more than 50% when deformation takes place at 900 ^{o}C. The minimum temperature at which dynamic transformation can take place in CP Ti grade 2 has also been determined in this way.

Experimental Procedure

1. Commercially pure titanium

A commercially pure titanium grade 2 (β-transus = 915 ^{o}C) was obtained from the McMaster Co. with the composition shown in Table 1. Cylindrical specimens 9 mm in height and 6 mm in diameter were machined from cylindrical rods.

2. Heat treatment

Samples were annealed at 800 ^{o}C for 1 h to homogenize the microstructure and remove any residual stresses [8,9]. A box furnace with an argon gas atmosphere was employed. Samples were finally air cooled to room temperature. Stainless steel envelopes were used to protect the samples from oxidation. With the aid of this procedure, an equiaxed microstructure was produced with an average grain size of 40 um. These results are similar to those reported in references [8,10,11]. This annealing process is illustrated schematically in **Fig. 1.**

3. Compression deformation tests

Hot compression tests were carried out on an MTS 100 kN machine, **Fig. 2**. The experiments were conducted at elevated temperatures using a radiant heating furnace under an argon protective atmosphere. The temperatures were measured using a thermocouple in contact with the sample. Deformation temperatures between 750 and 900 ^{o}C were used to study the effect of deformation below the b-transus. Tests between 930 and 970 ^{o}C were also carried out to determine the critical stress required to form the fresh beta phase at temperatures above the β-transus. To reduce the amount of oxygen absorbtion, a 5 C/s heating rate was used to reduce the absorbtion time. Samples were held at temperature for 2 min to ensure a homogenous temperature distribution throughout the specimen.

A schematic view of the MTS compression machine is presented in **Fig. 2**. Samples were deformed to a strain of 0.8 at a strain rate of 0.01 s-1. These were then water quenched to freeze the phases formed at each temperature. The deformation process is described schematically in **Fig. 3**.

4. Microstructural characterization

The deformed samples were investigated using optical microscopy. They were sectioned along their transverse axes and hand ground using silicon carbide papers with particle sizes of 320, 400, 600, and 800 mesh. Samples were polished using 3um and 1um diamond suspensions and finally etched for 10 s with a solution of 10 mL HF + 5 mL HNO_3 + 85 mL H_2O.

Results and Discussion

5. Flow stress

Stress-strain curves were generated from the hot compression tests at different temperatures leading to the flow curves shown in **Fig. 4**. Three of the temperatures were in the beta phase region and five below the β-transus. At 900 ^{o}C (15 ^{o}C below the β-transus), there is considerable flow softening. At this temperature, the driving force is high enough to convert 50% of the harder alpha phase into the softer beta phase. Such flow softening has also been observed by other authors, although this has generally been attributed to DRX or texture softening [2].

6. Microstructure

Beta phase formation began at 840 ^{o}C and led to the presence of 30% β as shown in Fig. 5-C. At 900 ^{o}C, more than 50% of martensite transformed beta was formed. The beta volume fractions formed by dynamic transformation at various temperatures below the β-transus were measured using the Image J software. These are plotted against temperature in **Fig.6**.

7. Driving force

The driving force for the transformation was calculated from the difference between the critical stress of the harder alpha phase and the yield stress of the softer fresh beta phase as seen in **Fig. 7**. This force is compared with the driving force for transformation proposed in reference [6], see **Fig. 8**. At 880 ^{o}C, the driving force of 288 J/mol is greater than the barrier energy of 65 J/mol. On the other hand, at 750 ^{o}C, the driving force of 378 J/mol is lower than the 565 J/mol obstacle energy that corresponds to this temperature [6].

8. The minimum temperature to induce transformation

Finally, the minimum temperature at which transformation can be induced was calculated from the peak stress and the critical stress calculated from the literature, see **Fig. 9**. The peak stress is employed here because it is an estimate of the stress required to initiate transformation into the beta phase.

Summary

Hot compression tests were carried out on commercially pure titanium grade 2. Dynamic transformation was observed to take place leading to the following conclusions:

- Dynamic transformation takes place in commercially pure titanium grade 2 when it is deformed at temperatures below the β transus.
- The driving force for the transformation is the flow stress difference between the work hardened α at the critical stress and the yield stress of the fresh β phase that takes its place. These driving forces fall in the range 200–500 J/mol.
- The obstacles to the transformation consist of the free energy difference between the two phases and the work of dilatation, both of which depend on temperature.
- At temperatures of 840, 860, 880, and 900 ^{o}C, the β volume fraction increases by 30, 32, 36, and 55%, respectively.
- The minimum temperature at which dynamic transformation can be induced in CP Ti Grade 2 is 765 ^{o}C. No dynamic transformation was observed below this temperature.

Acknowledgments

The authors acknowledge with gratitude funding received from the Natural Sciences and Engineering Research Council of Canada (NSERC) and the McGill Engineering Doctoral Award (MEDA) program (CAJr).

References

1- Koike, J., Shimoyama, Y., Ohnuma, I., Okamura, T., Kainuma, R., Ishida, K., & Maruyama, K. (2000). Stress-induced phase transformation during superplastic deformation in two-phase Ti–Al–Fe alloy. Acta Materialia, 48(9), 2059-2069.

2- Xu, C., & Zhu, W. (2010). Transformation mechanism and mechanical properties of commercially pure titanium. Transactions of Nonferrous Metals Society of China, 20(11), 2162-2167.

3- Jonas, J. J., Aranas Jr, C., Fall, A., & Jahazi, M. (2017). Transformation softening in three titanium alloys. Materials & Design, 113, 305-310.

4- Yang, H. S., Gurewitz, G., & Mukherjee, A. K. (1991). Mechanical Behavior and Microstructural Evolution during Superplastic Deformation of Ti-6Al-4V. Materials Transactions, JIM, 32(5), 465-472.

5- Zong, Y. Y., Shan, D. B., Xu, M., & Lv, Y. (2009). Flow softening and microstructural evolution of TC11 titanium alloy during hot deformation. Journal of Materials Processing Technology, 209(4), 1988-1994.

6- Aranas, C., Foul, A., Guo, B., Fall, A., Jahazi, M., & Jonas, J. J. (2017). Determination of the critical stress for the initiation of dynamic transformation in commercially pure titanium. Scripta Materialia, 133, 83-85.

7- Poliak, E. I., & Jonas, J. J. (1996). A one-parameter approach to determining the critical conditions for the initiation of dynamic recrystallization. Acta Materialia, 44(1), 127-136.

8- Zeng, Z., Zhang, Y., & Jonsson, S. (2009). Deformation behaviour of commercially pure titanium during simple hot compression. Materials & Design, 30(8), 3105-3111.

9- Hajizadeh, K., Eghbali, B., Topolski, K., & Kurzydlowski, K. J. (2014). Ultra-fine grained bulk CP-Ti processed by multi-pass ECAP at warm deformation region. Materials Chemistry and Physics, 143(3), 1032-1038.

10- Shinbine, A., Garcin, T., & Sinclair, C. (2016). In-situ laser ultrasonic measurement of the hcp to bcc transformation in commercially pure titanium. Materials Characterization, 117, 57-64.

11- Nemat-Nasser, S., Guo, W. G., & Cheng, J. Y. (1999). Mechanical properties and deformation mechanisms of a commercially pure titanium. Acta Materialia, 47(13), 3705-3720.

Figure captions

Figure 1. Annealing schedule of the machined CP Ti grade 2 samples.

Figure 2. Left: 100kN MTS machine used for performing compression tests. Right: Schematic of the 100kN MTS compression machine.

Figure 3. Thermomechanical schedule of the compression tests.

Figure 4. Stress-strain curves determined at eight different temperatures.

Figure 5. Optical micrographs show an increase in β-phase formation with increasing deformation temperature.

Figure 6. Comparison of the beta phase fraction in undeformed and deformed samples.

Figure 7. The $\boldsymbol{\sigma}$ (critical-hard phase) − $\boldsymbol{\sigma}$ (yield-soft phase) for the α → β transformation.

Figure 8. The driving force for the α → β transformation.

Figure 9. The minimum temperature to induce DT in CP Tfi Grade 2.

Table(s)

Table 1. Chemical composition (mass %) of CP Ti grade 2

Fe	C	H	O	N	Ti
≤0.30	≤0.10	≤0.015	≤0.25	≤0.03	Bal.

Figure(s)

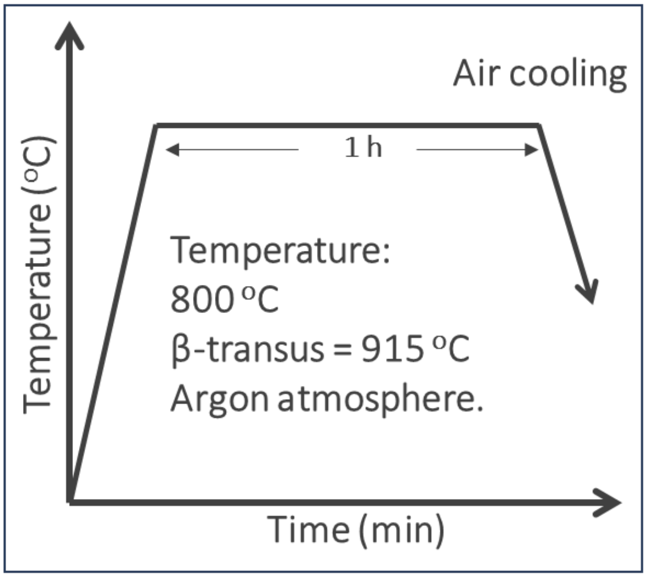

Figure 1. Annealing schedule of the machined CP Ti grade 2 samples.

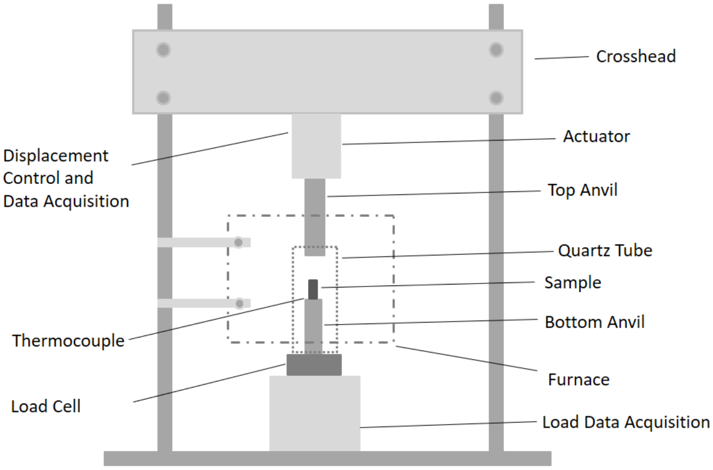

Figure 2. Schematic of the 100kN MTS compression machine.

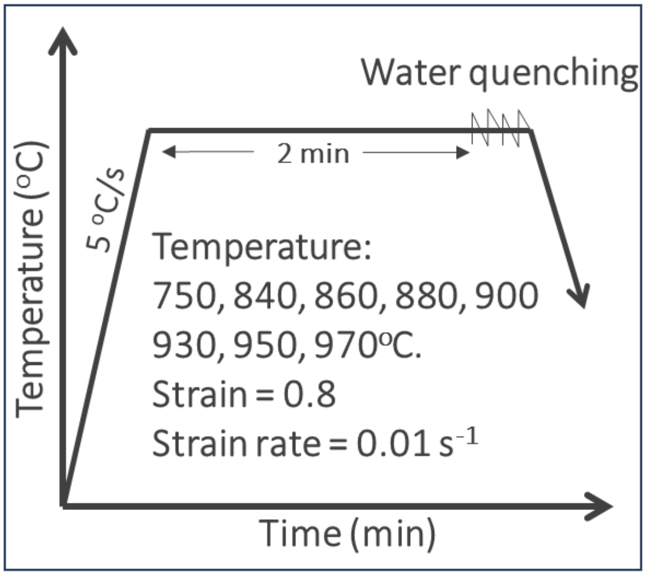

Figure 3. Thermomechanical schedule of the compression tests.

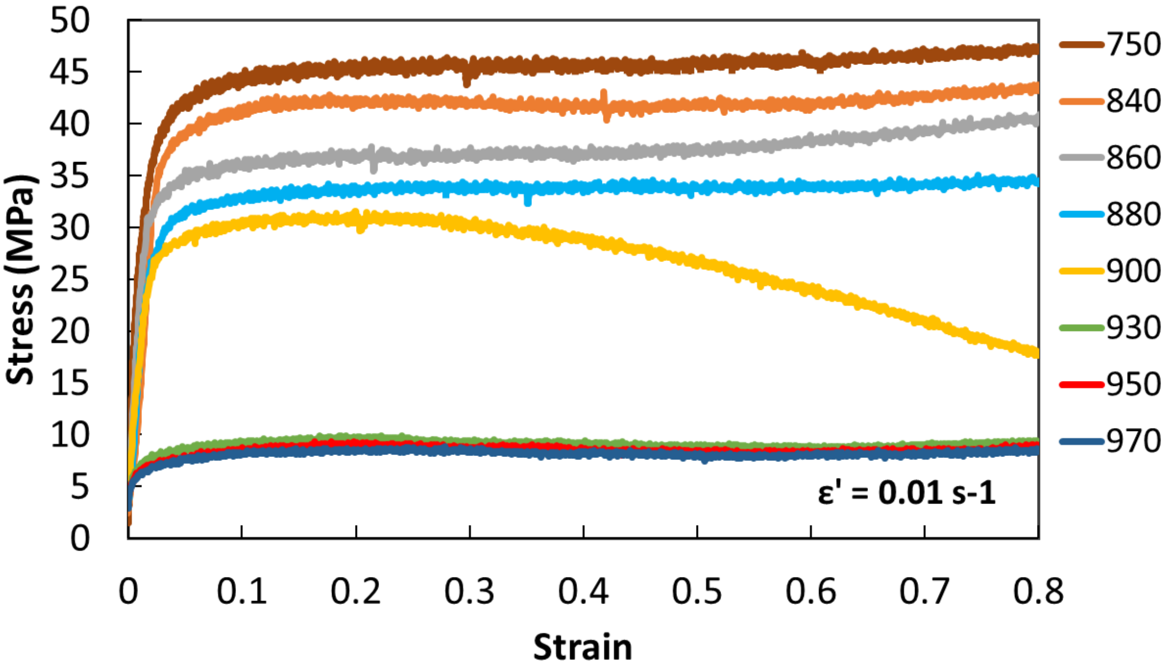

Figure 4. Stress-strain curves determined at eight different temperatures.

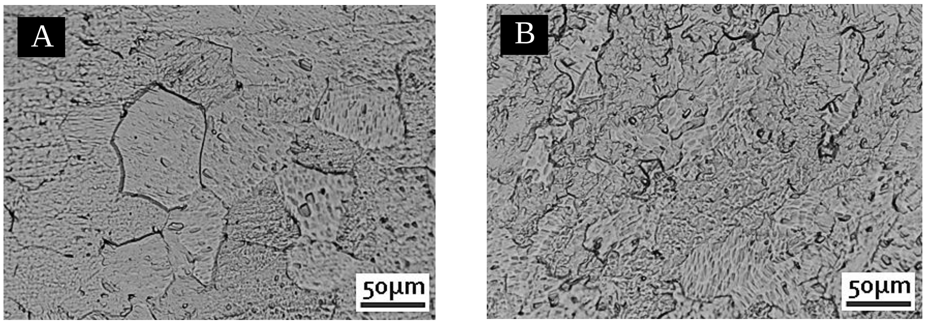

As received heat treated

750 ºC

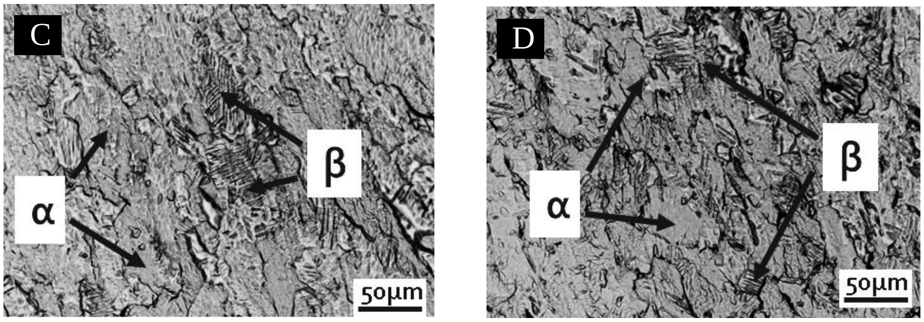

840 ºC

860 ºC

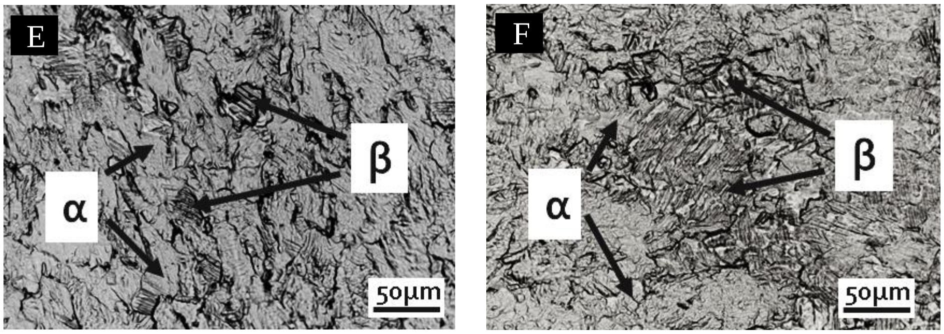

880 ºC

900 ºC

Figure 5. Optical micrographs show an increase in β-phase formation with increasing deformation temperature.

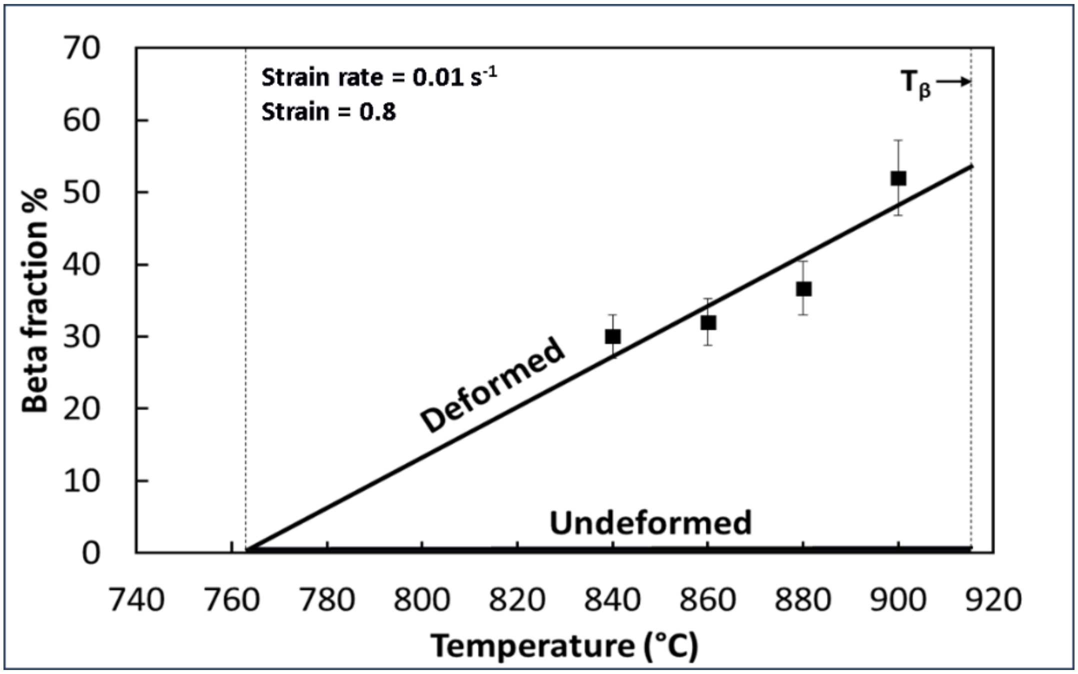

Figure 6. Comparison of the beta phase fraction in undeformed and deformed samples.

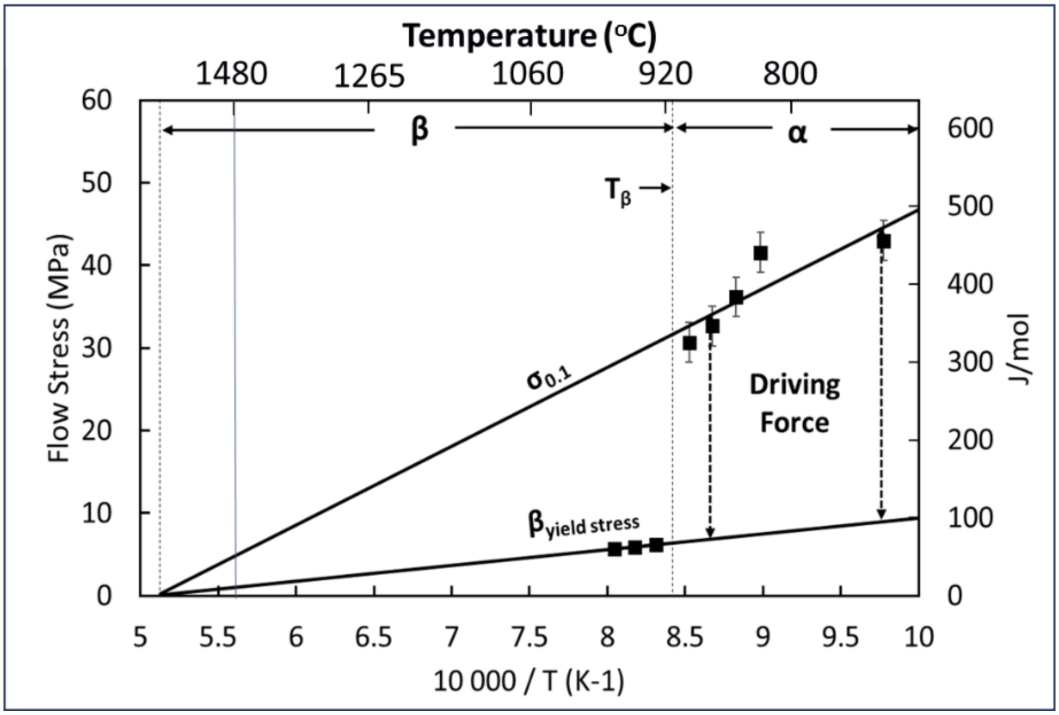

Figure 7. The ***σ*** (critical-hard phase) − ***σ*** (yield-soft phase) for the α → β transformation.

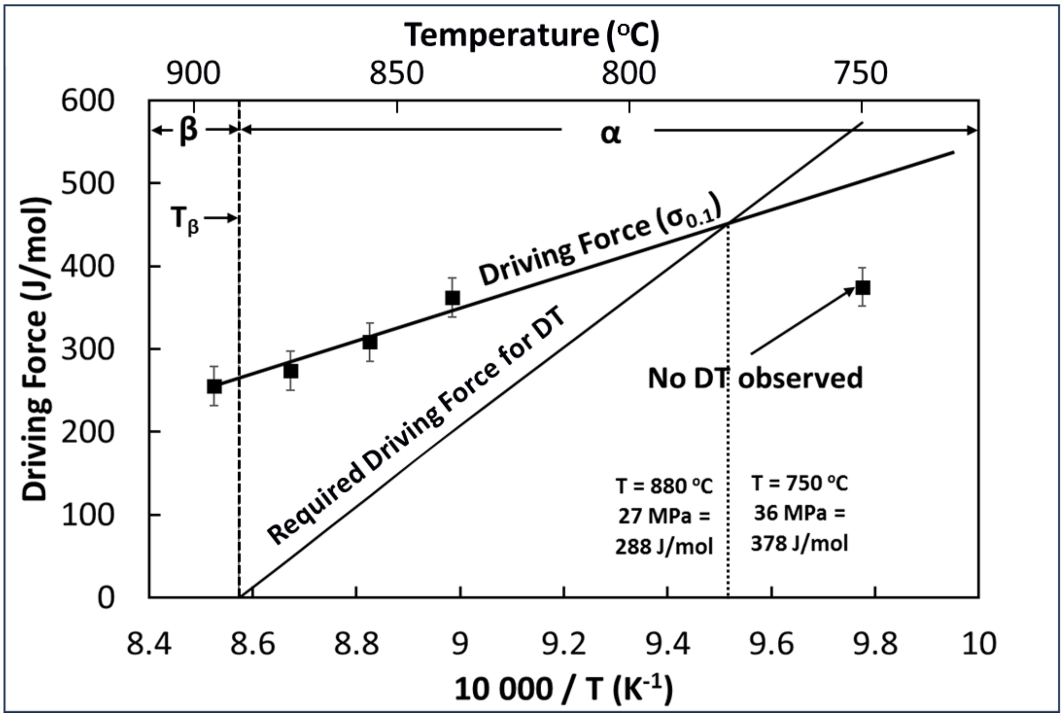

Figure 8. The driving force for the α → β transformation.

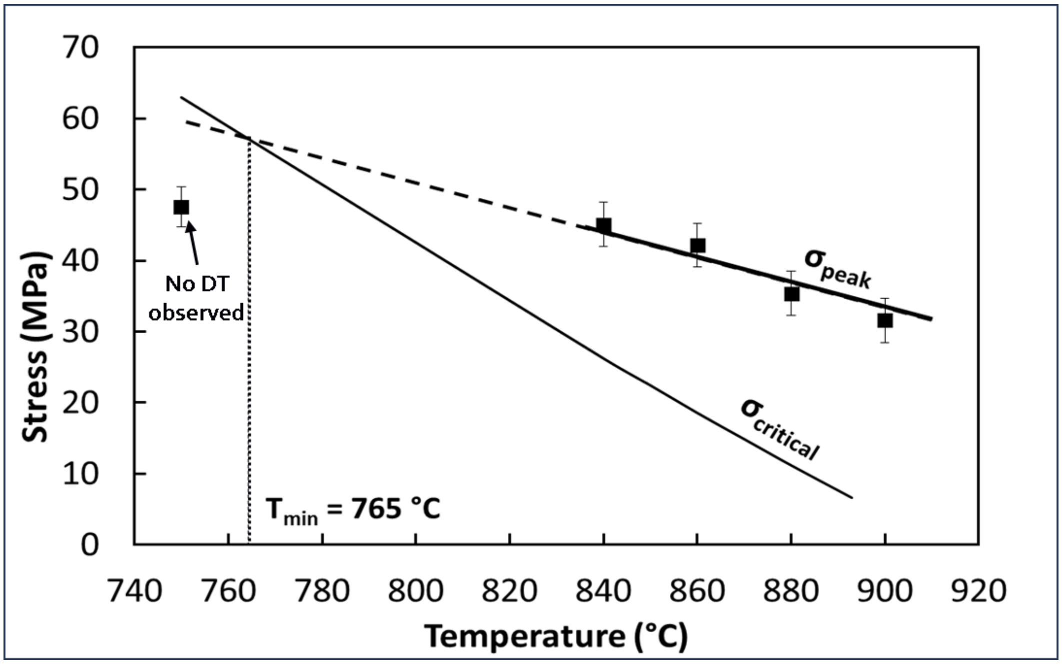

Figure 9. The minimum temperature to induce DT in CP Tfi Grade 2.